Advancements of carbon dots: From the perspective of medicinal chemistry

Shengtao Zhang, Li Shen, Pengyue Xu, Jiali Yang, Pengliang Song, Lifang Li, Yan Li, Yongmin Zhang, Shaoping Wu

Advancements of Carbon Dots: From the Perspective of Medicinal Chemistry

Shengtao Zhang[a,b,§], Li Shen[c,§], Pengyue Xu[a], Jiali Yang[a], Pengliang Song[a], Lifang Li[a], Yan Li[b,], Yongmin Zhang[b,d], Shaoping Wu[a,*]*

[a] *Key Laboratory of Resource Biology and Biotechnology in Western China, Ministry of Education, Biomedicine Key Laboratory of Shaanxi Province, Northwest University, 229 Taibai Road, Xi'an, Shaanxi, 710069, P. R. China.*

[b] *Key Laboratory of Synthetic and Natural Functional Molecule Chemistry of the Ministry of Education, College of Chemistry and Materials Science, Northwest University, Xi'an, Shaanxi, 710069, P. R. China.*

[c] *School of Pharmaceutical Sciences, Zhejiang Chinese Medical University, 310061, Hangzhou, China.*

[d] *Sorbonne Université, CNRS, Institut Parisien de Chimie Moléculaire, UMR 8232, 4 place Jussieu, 75005, Paris, France.*

[§] *These authors contributed equally to this work.*

[*] *Corresponding author: wushaoping@nwu.edu.cn*

Abstract

Carbon dots (CDs) exhibit great potential in medicinal chemistry due to its excellent optical properties, biocompatibility and scalability, which have attracted significant interest. Based on their specific synthesis and modification, this review provided an overview of the evolution of the synthesis of CDs and reviewed the discovery and development of their optical properties. This review examines recent advances of CDs in medicinal chemistry, with a particular focus on the use of CDs as drugs and carriers for photodynamic and photothermal therapies in the field of neurological disorders, cancer, bacterial, viral, and further in combination with imaging for diagnostic and therapeutic integration. Finally, this review addresses the challenges and limitations of CDs in medicinal chemistry. This review provides a

comprehensive overview of the development process of CDs and their applications in various aspects of medicinal chemistry, thereby offers insights to the development of CDs in the field of medicinal chemistry.

Keywords: Carbon Dots; Medicinal chemistry; Drug delivery; Drug analysis; Nanomedicine; Imaging

Contents

1. Introduction

Diseases have existed since ancient times, and the use of scientific and appropriate methods to treat them has been a long-standing question of mankind. Medicinal chemistry has developed from the original alchemists to the modern science for hundreds of years, but there are still many limitations in the use of drugs, for example, in cancer treatment, systemic nature of drugs could lead to great side effects [1, 2], excessive active pharmaceutical ingredients in living areas caused by drug abuse [3], rising bacterial resistance due to misuse of antibiotics [4, 5], difficulties in treating Central Nervous System (CNS) disorders due to the difficulty in getting drugs across the Blood-Brain Barrier (BBB) [6], lack of antiviral drugs, etc. [7, 8]. With the advancement of medicinal chemistry research, a number of nanomedicines beyond the scope of the five laws of drugs are being used for disease treatment or clinical research [9-11]. Nanomedicine focuses on nanomedicine production, drug delivery, drug analysis and imaging for targeted delivery, analytical

diagnosis and treatment. By combining nanomedicines with photodynamic therapy, photothermal therapy, phage therapy etc., significant progresses have been made in the diagnosis and treatment of cancers, brain diseases, antiviral and antibacterial [12-17]. An excellent nanomedicine must have the following characteristics: good therapeutic effect on diseases, proper targeting and low side effects, etc. For the carrier to transport the drug, it must have the ability to bind to the drug, proper controlled release, low toxicity and high stability.

The discovery of Quantum Dots (QDs) is very important as it gives color to the nanomaterials and gives them fluorescent properties unlike the previous ones. The Quantum Confinement Effect (QCE) has given QDs unique optical properties that allow their fluorescence to be easily tuned by simply adjusting the size of the QDs, and QDs is considered to be the next generation of fluorescent materials [18]. Conventional semiconductor QDs have good optical properties, but their biological applications were limited due to high toxicity. Carbon Dots (CDs) not only inherits the excellent optical properties of QDs, but also has low toxicity and good biocompatibility, which is considered promising for biological applications [19]. CDs was first reported by Xu et al. in 2004 (Fig. 1) [20], but it was not formally identified as CDs until two years later [21]. The number of articles on CDs had grown steadily during this period and entered a period of rapid growth since 2012. The large number of articles on CDs are closely related to its excellent properties, such as emission-dependent excitation, up-conversion luminescence, Aggregation-Induced

Emission (AIE), high fluorescence Quantum Yields (QDs), tunable fluorescence wavelengths, resistance to photobleaching and photo blinking [22]. CDs possess good biocompatibility and the literature reported that even at a high concentration of 2.0 mg/mL, cell toxicity remains low, which is a great advantage in bioimaging and as a drug [23]. CDs have been applied to nanomedicine, such as enhancing drug treatment effects through photodynamic therapy and photothermal therapy, delivering drugs to the target site for precision therapy, preparing CDs crossing the BBB for CNS disease treatment, and reducing bacterial resistance. In conclusion, CDs as a new type of nanomaterials, has a wide range of applications in medicinal chemistry, and its unique properties makes it attracted much attention in drug research and biomedical applications. Based on the applications of CDs in medicinal chemistry, this paper reviewed the preparation methods, optical properties of CDs and its applications in nanomedicines, drug carriers, drug analysis and imaging, as well as some challenges still exist. While the comprehensive applications of CDs in biomedicine have been previously reported, this review focuses on the use of CDs for therapeutic and diagnostic purposes in different disease scenarios based on specific synthesis or modification of CDs. It also examines the various applications, the process of development and the future of CDs in medicinal chemistry.

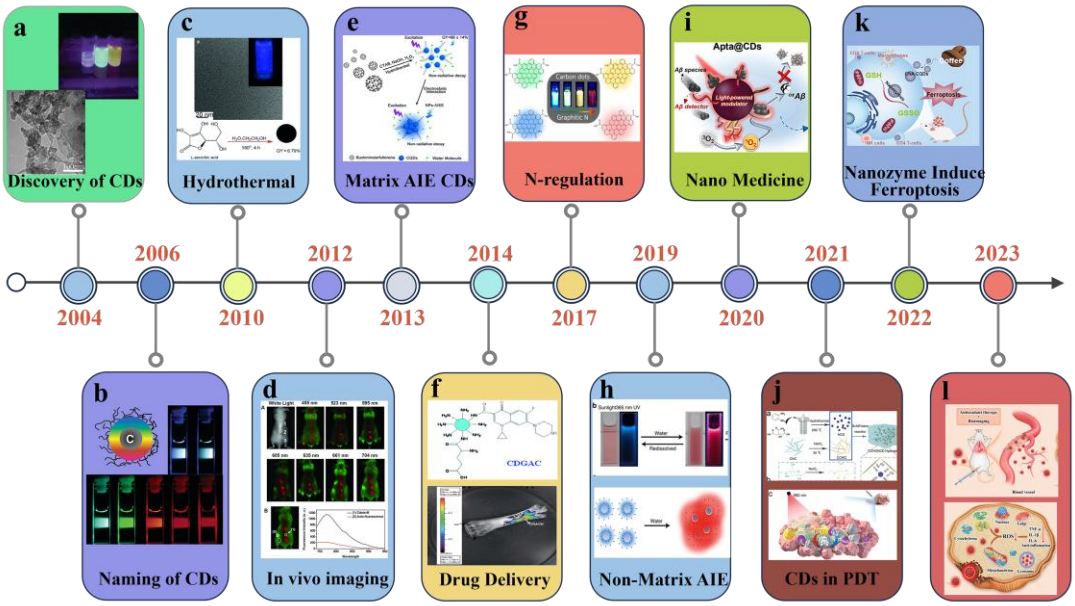

Fig. 1. Evolution of CDs and their use in medicinal chemistry. (a) Fluorescence and transmission electron microscopy images of the first discovered CDs. Reproduced with permission from ref [20]. Copyright 2004 American Chemical Society. (b) CDs named for the first time: the excitation-dependent properties of CDs. Reproduced with permission from ref [21]. Copyright 2006 American Chemical Society. (c) CDs was prepared for the first time by a hydrothermal method. Reproduced with permission from ref [24]. Copyright 2010 Wiley-VCH. (d) CDs was used for in vivo imaging firstly. Reproduced with permission from ref [25]. Copyright 2012 Wiley-VCH. (e) Preparation of CDs with AIEE properties by matrix doping method. Reproduced with permission from ref [26]. Copyright 2013 The Royal Society of Chemistry. (f) CDs for bone fracture detection and transport of therapeutic drugs. Reproduced with permission from ref [27]. Copyright 2014 The Royal Society of Chemistry. (g) Preparation of multicolored CDs by changing the nitrogen content. Reproduced with permission from ref [28]. Copyright 2017 American Chemical Society. (h) Preparation of matrix-free AIE CDs by modulating the structure of precursor. Reproduced with permission from ref [29]. Copyright 2019 Springer Nature. (i) CDs as nanomedicines for cancer treatment. Reproduced with permission from ref [30]. Copyright 2020 American Chemical Society. (j) CDs as photodynamic therapy drugs for cancer treatment. Reproduced with permission from ref [31]. Copyright 2021 Wiley-VCH. (k) CDs as nanozymes to induce iron apoptosis for cancer treatment. Reproduced with permission from ref [32]. Copyright 2022 American Chemical Society. (l) CDs for simultaneous imaging and treatment of acute liver injury. Reproduced with permission from ref [33]. Copyright 2023 Wiley-VCH.

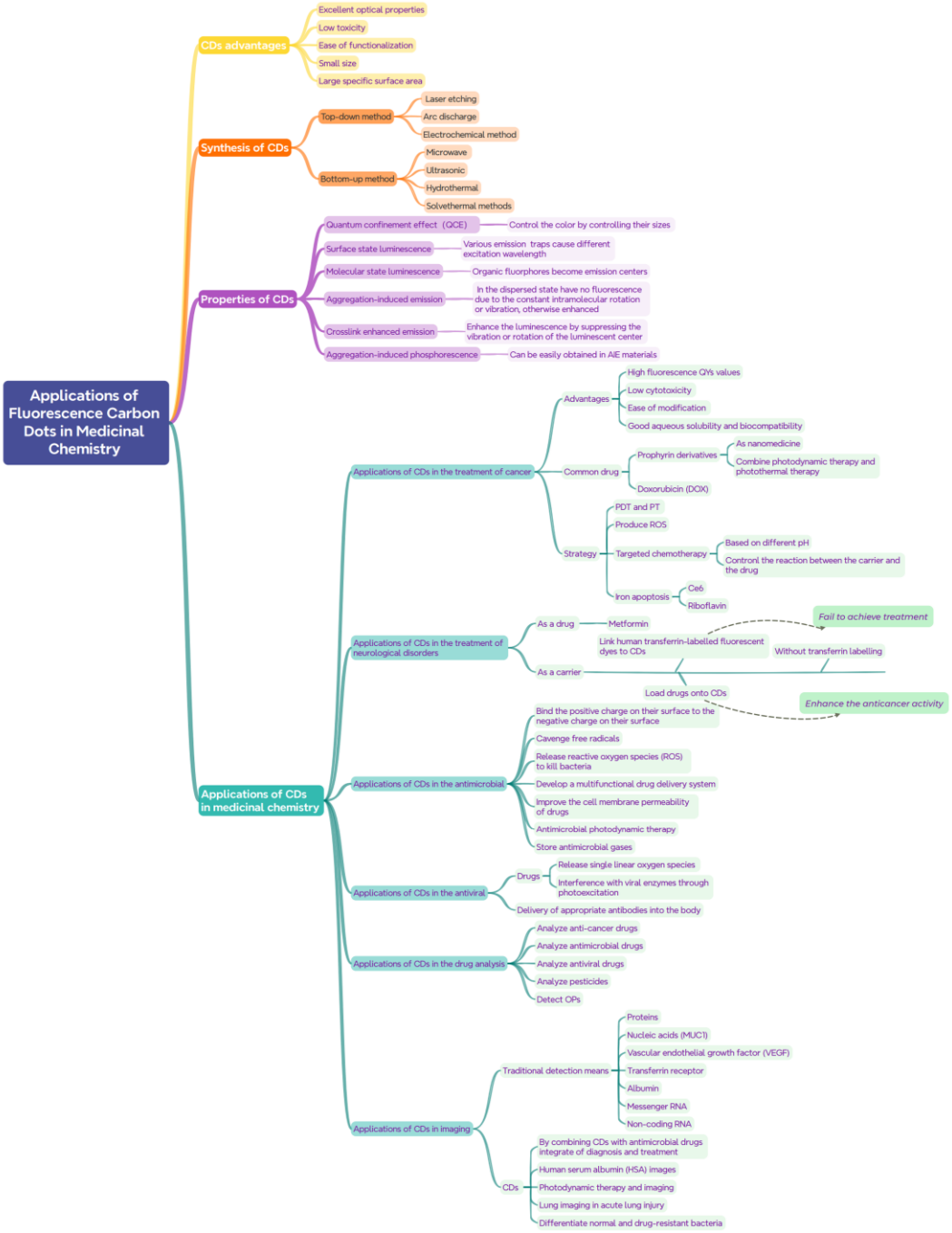

Scheme 1. Mind map of the recent research on applications of fluorescence CDs in medicinal chemistry.

2. Synthesis of CDs

2.1. Top-Down Method

The synthetic methods of CDs are divided into top-down and bottom-up method. The top-down method include laser etching [20], arc discharge [34] and

electrochemical [35], while the bottom-up method include microwave [36], ultrasonic [37], hydrothermal [38] and solvothermal [39]. CDs was first discovered by Xu's group when they purified single-walled Carbon Nanotubes (CNTs) with a high-energy pulsed laser beam, a method known as laser etching (Fig. 2a) [20]. The arc discharge method was also the main method for CDs preparation in the early period, Chaitoglou et al. designed an arc discharge reactor to improve the collection process of nanoparticles and obtained CDs with controllable and adjustable size (Fig. 2b) [34]. Compared with laser etching and arc discharge methods, the electrochemical method for preparing CDs has the advantage of low cost. Chang et al. prepared CDs through the process of electrooxidation, electropolymerization, carbonization and passivation, then obtained CDs with emission-dependent excitation properties and pH-sensitivity (Fig. 2c) [35]. In summary, the top-down methods above require high energy or strong acid and hard alkali, which need higher cost and the yield of CDs prepared were quietly low. Nevertheless, top-down CDs have higher crystallinity and excellent properties. In contrast, bottom-up CDs sometimes exhibit an amorphous nucleation structure.

2.2. Bottom-Up Method

Due to the shortcomings of the top-down method, the bottom-up method become main synthesis method gradually. High-quality CDs could be obtained by low-cost raw materials and simple instrumentation, making CDs a promising optical material. Recently, Hu's group synthesized solid-state CDs with a high Quantum Yields (QYs)

of 58.35% using the microwave method which exhibited emission-independent excitation, and this CDs was applied in white light-emitting diodes after combining with blue light-emitting chips (Fig. 2d) [40]. Jiang et al. synthesized a long-lived Room-Temperature-Phosphorescence (RTP) CDs using microwave heating of ethanolamine and phosphoric acid, the gram-level CDs was expected to be used for practical applications [41]. The ultrasonic method attracted the attention of researchers because of its simple operation and short time-consuming. Li et al. synthesized glucose-derived CDs with Near-infrared (NIR) and up-conversion luminescence, which show a great potential in biological applications (Fig. 2e) [42]. Compared with microwave and ultrasonic methods, hydrothermal synthesis of CDs only requires a set of reactors and a heating device, which has the advantages of mild conditions and environmental friendliness. Liu et al. synthesized a fluorescent CDs with NIR emission by hydrothermal method using mulberry leaves as raw material, which has an extremely narrow half-peak width (20 nm), and the QDs reached 73%. By feeding the silkworms the CDs, the silkworms and the silk produced can emit red fluorescence, and the survival rate of the silkworms fed with the CDs was close to 100%, which is expected to be used in the silk industry [43]. Solvothermal method employed other solvents to replace water and the solvent will directly participate in the reaction, providing more expandability of CDs. Huo et al. prepared multicolored CDs using a solvothermal method and found that the fluorescence of CDs synthesized in the same solvent gradually red-shifted as the degree of surface state oxidation

increased (Fig. 2f) [38]. In summary, the bottom-up method has advantages of simple synthesis, low cost, high quality and high yield. It exhibits great potential in practical application, which is the principal method of synthesizing CDs at present.

A number of unconventional methods to prepare CDs were documented. When subjected to an appropriate alternating magnetic field (AMF), the magnetic nanoparticles are capable of generating heat, thereby externally triggering a burst of chemical reactions. Zhu et al. employed a magnetic hyperthermia (MHT) technique to synthesis blue, green and yellow CDs on a large scale within one hour. These CDs exhibited excellent monodispersity and solubility in water [44]. The continuous hydrothermal flow synthesis (CHFS) process exploits the significant density differential between the precursor solution and supercritical water, enabling rapid mixing and establishing homogeneous conditions for reaction kinetics and particle growth. Kellici et al. employed a CHFS approach to synthesize N-doped CDs in fractions of a second, demonstrating the great potential for rapid synthesis of CDs [45]. In recent times, machine learning (ML) has been the subject of considerable interest as a highly effective and adaptable tool. Han et al. employed ML to successfully predict and optimize the synthesis process of CDs, and developed a regression ML model for hydrothermal synthesis of CDs, which can be used to guide the synthesis of high-quality CDs [46].

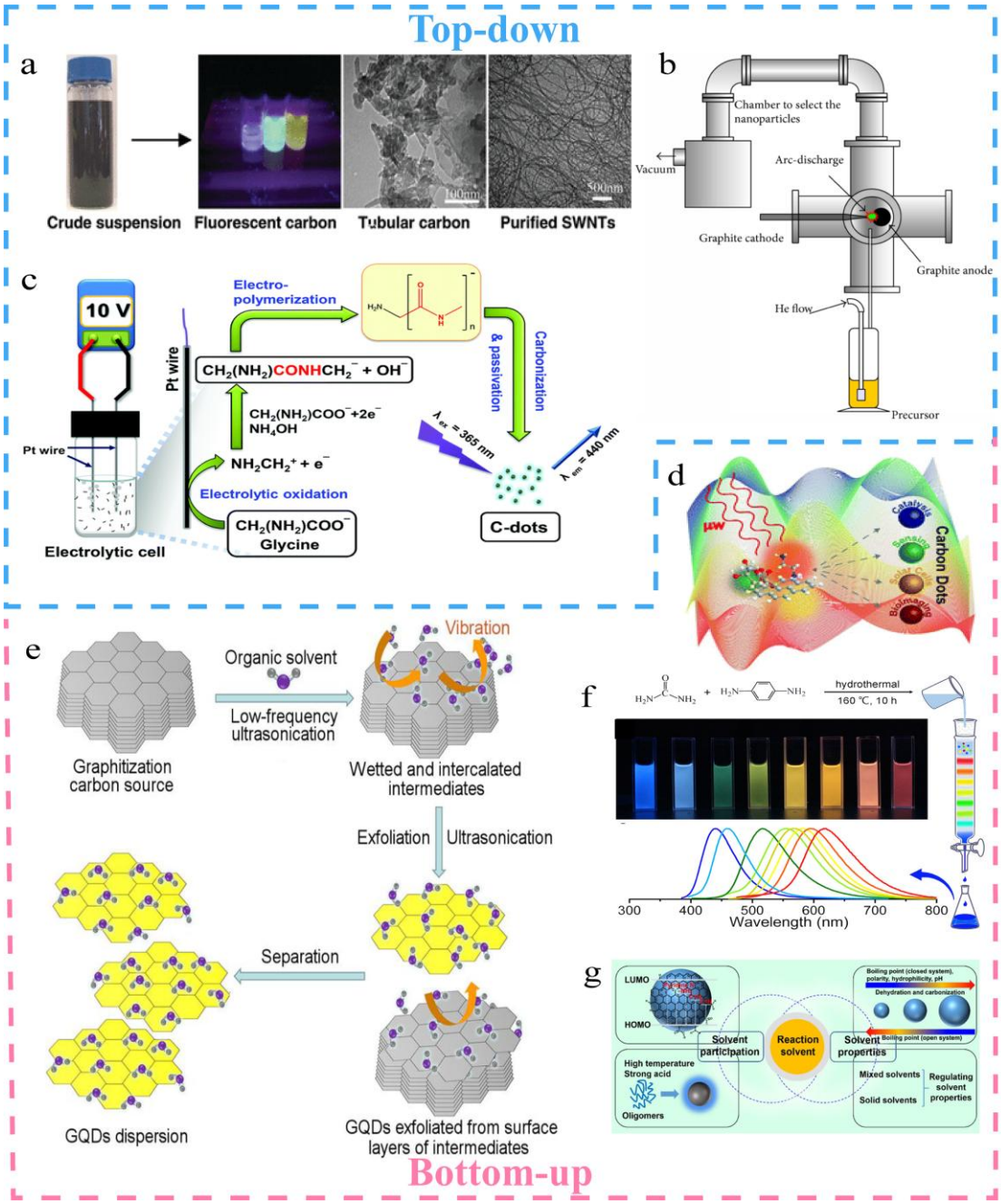

Fig. 2. Synthetic methods of CDs. Top-down methods include: (a) Laser etching. Reproduced with permission from ref [20]. Copyright 2004 American Chemical Society. (b) Arc discharge. Reproduced with permission from ref [34]. Copyright 2014 Hindawi Publishing Corporation. (c) Electrochemical method. Reproduced with permission from ref [35]. Copyright 2014 The Royal Society of Chemistry. Bottom-up methods include: (d) Microwave Reproduced with permission from ref [36]. Copyright 2019 The Royal Society of Chemistry. (e) Ultrasonic. Reproduced with permission from ref [37]. Copyright 2016 Elsevier. (f) Hydrothermal Reproduced with permission from ref [38]. Copyright 2016 American Chemical Society. (g) Solvothermal methods. Reproduced with permission from ref [39]. Copyright 2023 Elsevier.

3. Properties of CDs

3.1. Quantum Confinement Effect

QCE was proposed by Kubo in his study of metallic nanoparticles. When the size of a particle reaches the nanoscale, the electron energy level near the Fermi energy level splits from the continuum state into a two-split energy level. Since the size of the QDs is close to the Bohr radius of the exciton, the motion of the carriers will be limited as the size decreases, leading to an increase in kinetic energy, which in turn leads to an increase in the effective band gap of the QDs. According to the photon energy formula, the emission wavelength will decrease with the increase of the bandgap, in other words, the emission wavelength will blue-shift as the size of the QDs decreases, and *vice versa*, the emission wavelength will red-shift (Fig. 3a) [47]. Accordingly, researchers regulate the fluorescent color of CDs by adjusting their sizes. Tian et al. synthesized CDs using different solvents from citric acid and urea with diameters of 1.7 nm, 2.8 nm and 4.5 nm, emitting blue, green and red fluorescence, respectively, proving the existence of QCE in CDs [48].

3.2. Surface State Luminescence

Fluorescence is a photoluminescence phenomenon. When a fluorophore absorbs a certain wavelength of light, its electrons jump from the ground state to the excited state, and then reaching the lowest excited state by internal transition and continued to return to the ground state while emitting fluorescence. Regardless of the excitation wavelength chosen, for the same fluorescent substance electrons will jump to the

lowest excited state. Therefore, the fluorescence wavelength of conventional fluorescent dyes will not be affected by the wavelength of the excitation light. However, it is different in CDs that the abundance of emission traps gives CDs the excitation-dependent properties. The shift of excitation wavelengths will change the fluorescence of CDs due to their various emission traps. The characteristic was used for multi-color imaging to meet the needs of different application environments. Li et al. synthesized emission-dependent excitation CDs using dried astragalus as raw material, and achieved multi-color cellular imaging by simply changing the excitation wavelength [49]. The degree of oxidation on the surface of the CDs will also affect the properties of CDs. Ding et al. synthesized eight colors of CDs by a one-pot hydrothermal method and separated them with silicone columns (Fig. 3b). Transmission electron microscopy showed that these CDs were similar in size and carbon nucleus structure, whereas X-ray photoelectron spectroscopy (XPS) showed that the amount of C-N, C-O and C=O gradually increased with the redshift of fluorescence, which was consistent with the degree of oxidation [38]. Defect states will also affect the fluorescence of CDs. The defects on CDs will make the excitons of CDs jump to the defect energy level and then return to the ground state, which increases the relaxation and binding path of excitons. In 2006, Sun et al. synthesized CDs by laser etching of a carbon target, the large number of defects on the surface of the CDs resulted in weak luminescence after treatment of CDs with nitric acid, whereas bright fluorescence emission was observed after the addition of the

passivator (polyethylene glycol PEG1500) [21].

3.3. Molecular State Luminescence

Different from surface state luminescence, molecular state luminescence refers to organic fluorophores on the surface of CDs that become emission centers. Molecular-state luminescent CDs are generally synthesized by a bottom-up method, in which carbon nuclei is formed after high-temperature dehydration and carbonization, and unreacted raw materials or newly generated fluorophores embedded in the carbon nuclei become emission centers, which exhibit high stability and weak fluorescence emission behavior. In 2015, Song et al. prepared molecular state luminescent CDs from citric acid and ethylenediamine, which demonstrated the existence of molecular state luminescence by the similarity of fluorescence properties with the constructed imidazo [1,2]pyridine-7-carboxylic acid, 1,2,3,5-tetrahydro-5-yloxy (IPCA) [50]. Coincidentally, Cao et al. synthesized CDs from o-phenylenediamine and obtained five CDs by silica gel column separation in 2022, among which yellow CDs and green CDs were related to 2,3-diaminophenazine (DAP) and 2-amino-3-hydroxyphenazine (AHP), respectively. The Mass Spectrometry (MS) and Nuclear Magnetic Resonance (NMR) proved the presence of DAP and AHP, which provided conclusive evidence for the molecular state luminescence of CDs (Fig. 3c) [51].

3.4. Aggregation-Induced Emission

Due to the strong π-π stacking effect and excessive energy transfer, conventional

fluorescent CDs undergo Aggregation-caused quenching (ACQ) in the aggregated state, which greatly limits their applications. In 2013, Gao's group found that modification of alkyl long chains on the surface of CDs could inhibit the ACQ of CDs, which led to the study of AIE of CDs [26]. Hu et al. discovered AIE phenomenon in CDs synthesized with 2,2’-Dithiosalicylic acid as raw materials in 2019, and proposed a mechanism that fluorescence of carbon core of CDs behave ACQ, while surface state luminescence with disulfide bond exhibits AIE properties (Fig. 3d) [29].

3.5. Crosslink Enhanced Emission

Crosslink enhanced emission (CEE) is a kind of fixed effect produced by crosslinking, which enhances the luminescence by suppressing the vibration or rotation of the luminescent center. In recent years, carbonated polymer dots (CPDs) have emerged as a new member of CDs family. CPDs exhibits no defined chemical structure, a polymer cross-linking or hybrid lattice structure on the inside and a hydrophilic functional group or polymer chain on the outside. In 2014, Zhu et al. proposed CEE in CDs for the first time, and they synthesized CPDs from non-conjugated branched polyethyleneimine and carbon tetrachloride, investigated the relationship between its structure and spectral properties, and found that CEE was a key factor in the luminescence properties. In the polymer lattice, the vibration or rotation of the CPDs is suppressed and the non-radiative transitions are reduced, resulting in fluorescence enhanced (Fig. 3e). In contrast to AIE, under high temperatures or high-power UV lamps, the vibration and rotation of CPDs are

intensified, which increases the non-radiative transitions and thus quenches its fluorescence [52]. CPDs based on CEE inherits the stability and biocompatibility of CDs as well as the advantages of tunable fluorescence and good water solubility, which make it a promising new material [53].

3.6. Aggregation-Induced Phosphorescence

Phosphorescence and fluorescence are both photoluminescence phenomena, the difference being that the excited state electrons will jump from the first excited singlet state to the first excited triplet state through intersystem crossing, then from the first excited triplet state to the lowest vibrational energy level through vibrational relaxation, and finally to the ground state, accompanied by phosphorescence [54]. Due to the special properties of phosphorescence, phosphorescent materials are widely used in the fields of anti-counterfeiting, sensing, bio-imaging and optical devices. It has been shown that in a rigid structure, the movement of CDs is restricted, thus emitting phosphorescence, thus CDs with phosphorescent properties can be easily obtained in AIE materials [55-58]. Wang et al. synthesized CDs that emit phosphorescence in water by directly calcining 1,2,4-triaminobenzene in the presence of inorganic salts, which has AIE properties in water, and phosphorescence was appeared due to the combined effect of crystalline confinement and AIE (Fig. 3f) [59]. A recent work reported a method to synthesis full color RTP CDs at wavelengths between 453-632 nm, which exhibits stability afterglow due to the multiple constraints of hydrogen bonding, covalent bonding and physical immobilization [60].

Some CDs can even emit phosphorescence in water. Li et al. prepared host-guest composites by pyrolysis of CNDs and cyanuric acid to achieve phosphorescence in water. The rigidity of the composites was enhanced by a water-induced rigid hydrogen bonding network of CDs, which suppressed nonradiative decay, improved RTP performance, and finally demonstrated in vivo/in vitro biomedical imaging capabilities [61].

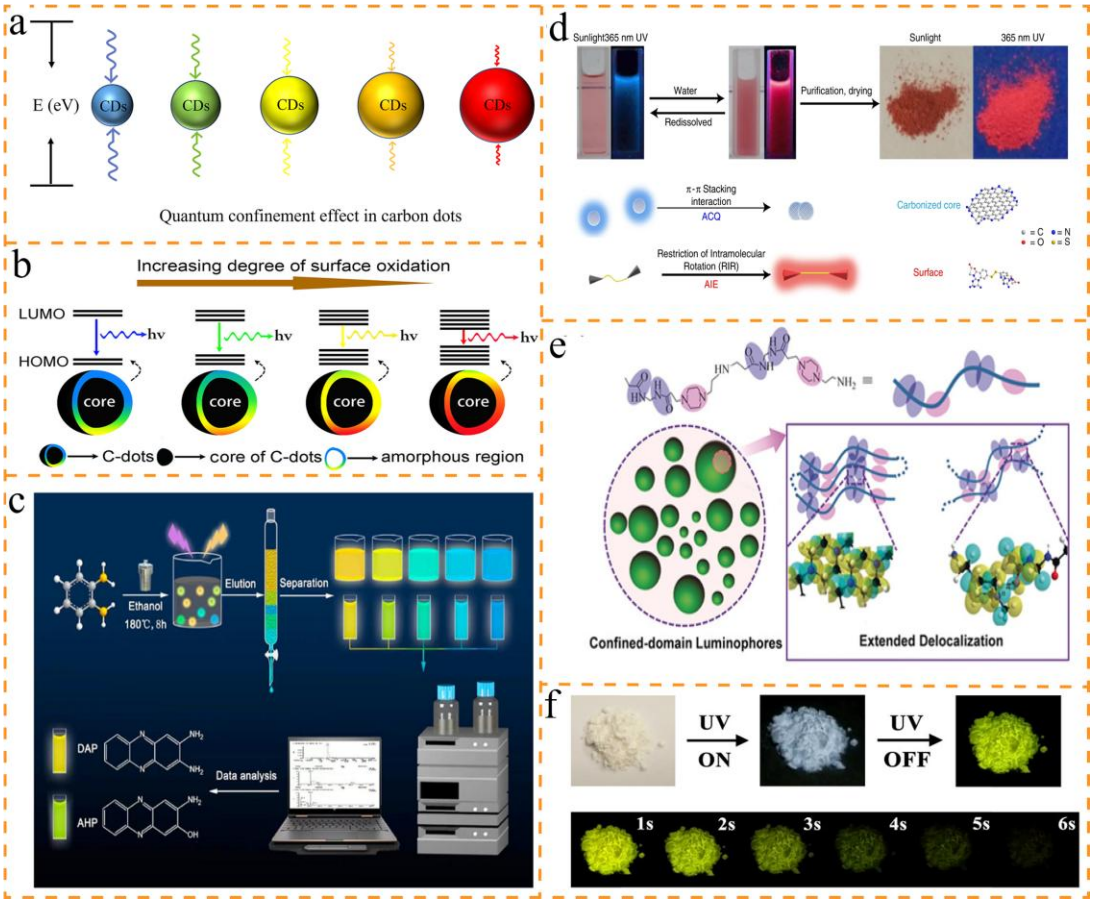

Fig. 3. Luminescence mechanism of CDs. (a) QCE of CDs. (b) Surface state luminescence of CDs. Reproduced with permission from ref [38]. Copyright 2016 American Chemical Society. (c) Molecular state luminescence of CDs. Reproduced with permission from ref [51]. Copyright 2022 Elsevier. (d) AIE properties of CDs. Reproduced with permission from ref [29]. Copyright 2019 Springer Nature. (e) CEE of CDs. Reproduced with permission from ref [53]. Copyright 2015 Springer. (f) Aggregation-induced phosphorescence of CDs. Reproduced with permission from ref [59]. Copyright 2020 American Chemical Society.

4. Applications of CDs in Medicinal Chemistry

The term of nanomedicine has emerged in the 21st century to describe pharmaceuticals of a nano-scale. The emergence of nanomedicines aims to address the disadvantages of conventional medicine include low target specificity, poor biocompatibility, and toxic side effects [9, 10]. Despite the utilization of nanoparticles in therapeutic applications, they remain constrained by three significant limitations: poor water solubility, high toxicity and susceptibility to photobleaching. It is therefore imperative that nanoparticles are developed which can overcome these shortcomings. In this context, CDs display considerable potential. Firstly, CDs exhibit excellent biocompatibility and minimal toxicity to biological tissues. Secondly, the size and surface properties of CDs can be adjusted easily, enabling them to perform specific functions in nanomedicine, imaging, drug delivery and analysis. Thirdly, some CDs exhibit photosensitivity and have been employed in photodynamic therapy (PDT) and photothermal therapy (PT) by releasing reactive oxygen species (ROS) or other active substance. Lastly, the cost of CDs in preparation and application is relatively low, which helps to reduce the cost of therapy [62]. This section presents a review of the applications of CDs in anticancer therapy, the treatment of CNS diseases, antibacterial and antiviral therapy, drug analysis, and imaging.

4.1. Applications of CDs in the Treatment of Cancer

Cancer represents one of the most significant health concerns today, with a profound impact on human lives. Therefore, timely detection and treatment are

urgently needed. Cancer cell is transformed from normal cell, which can escape capture by the body's immune system and are difficult to destroy, hence cancer patients are often at risk of recurrence. CDs was used to treat cancer through PDT and PT, exhibiting negligible toxicity to cell. In the absence of light, CDs produce ROS, such as $^1O_2$, ·OH, which can kill cancer cell and deplete glutathione through redox methods. Furthermore, researchers focus on targeted chemotherapy, a form of low-toxicity chemotherapy that combines drugs with nanomaterials to deliver them to cancerous tissue without affecting other normal cell for precision treatment. The high fluorescence QYs values, low cytotoxicity, ease of modification, good water solubility and biocompatibility of CDs render it a strong candidate for drug delivery [1].

Porphyrin derivatives are employed as photosensitizers for the treatment of cancers [14, 63, 64]. Porphyrin-based CDs retained their anticancer activity and were used as nanomedicines to enhance the efficacy of light-based cancer treatments. Li et al. synthesized porphyrin-based CDs (TPP CDs) from TPP and chitosan, which could effectively generate ROS under light-emitting diode irradiation (6 $mW \cdot cm^2$). This was evidenced by absorption spectra and a single linear oxygen-indicating fluorescent probe (Fig. 4a) [14]. Following a 60-minute incubation period, the majority of HepG2 cell exhibited signs of death following the co-incubation of TPP CDs under light-emitting diode irradiation (16 $mW \cdot cm^2$). To further substantiate its therapeutic efficacy *in vivo*, a mouse model of hepatocellular carcinoma was established. The results showed that the tumor volume of mice injected with TPP CDs and irradiated

with light was significantly smaller than the control group, thereby confirming the anticancer potential of TPP CDs.

Additionally, CDs have been employed for cancer treatment by combining photodynamic therapy and photothermal therapy, Sun et al. immobilized traces of the photosensitizer Chlorin e6 (Ce6) on amino-rich red CDs (RCDs). The PT properties of RCDs (46.00%) and the PDT of Ce6 could be simultaneously activated under a 671 nm NIR laser to realize combined therapy (Fig. 4a) [62]. Li et al. synthesized CDs by using Ce6 and polyethylene as precursors, which was used as a phosphorescence initiator and treat cancer by generating ROS (Fig. 4b) [63]. Subsequently, CDs-Ce6 was obtained by modifying Ce6 to CDs, and then Cu^{2+} was introduced to CDs-Ce6 to obtain environmentally sensitive nanoparticles (NPs). These NPs undergo fluorescence quenching in the aggregate state, while restored after enter tumor cell. *In vitro* tests demonstrated that activatable fluorescence imaging and ROS therapy have a strong killing effect on tumor cell [64].

Iron apoptosis represents an efficacious cancer treatment strategy, is an oxidative stress-dependent cell death. This process is initiated by the depletion of glutathione, which in turn leads to the inactivation of glutathione peroxidase. This results in the accumulation of ROS and the promotion of immune activation, cellular iron apoptosis and promotion of immune, which can be used as an effective strategy for cancer therapy. Yao et al. prepared CDs by hydrothermal method using chlorogenic acid from coffee as a raw material, which can act as oxidized glutathione peroxidase and

catalyze the reduction of reduced glutathione to oxidized glutathione, through which unbalanced oxidation can induce cellular iron apoptosis and inhibit tumor growth. This process also activates the immune microenvironment of the tumor, demonstrating the prospect of application of CDs in medicine (Fig. 4d) [32]. Riboflavin has also been employed in the synthesis of green fluorescent CDs, which exhibit a significantly higher single-linear oxygen yield than riboflavin. In vivo testing demonstrated a notable reduction in tumor cell weight in mice when illuminated with light and CDs. It is therefore necessary to develop methods of utilizing the natural vitamin riboflavin as a photosensitizer for the treatment of cancer (Fig. 4e) [65]. Although CDs have shown considerable potential for the treatment of cancer, further studies and clinical trials are required to substantiate these findings and assess the feasibility of their practical application.

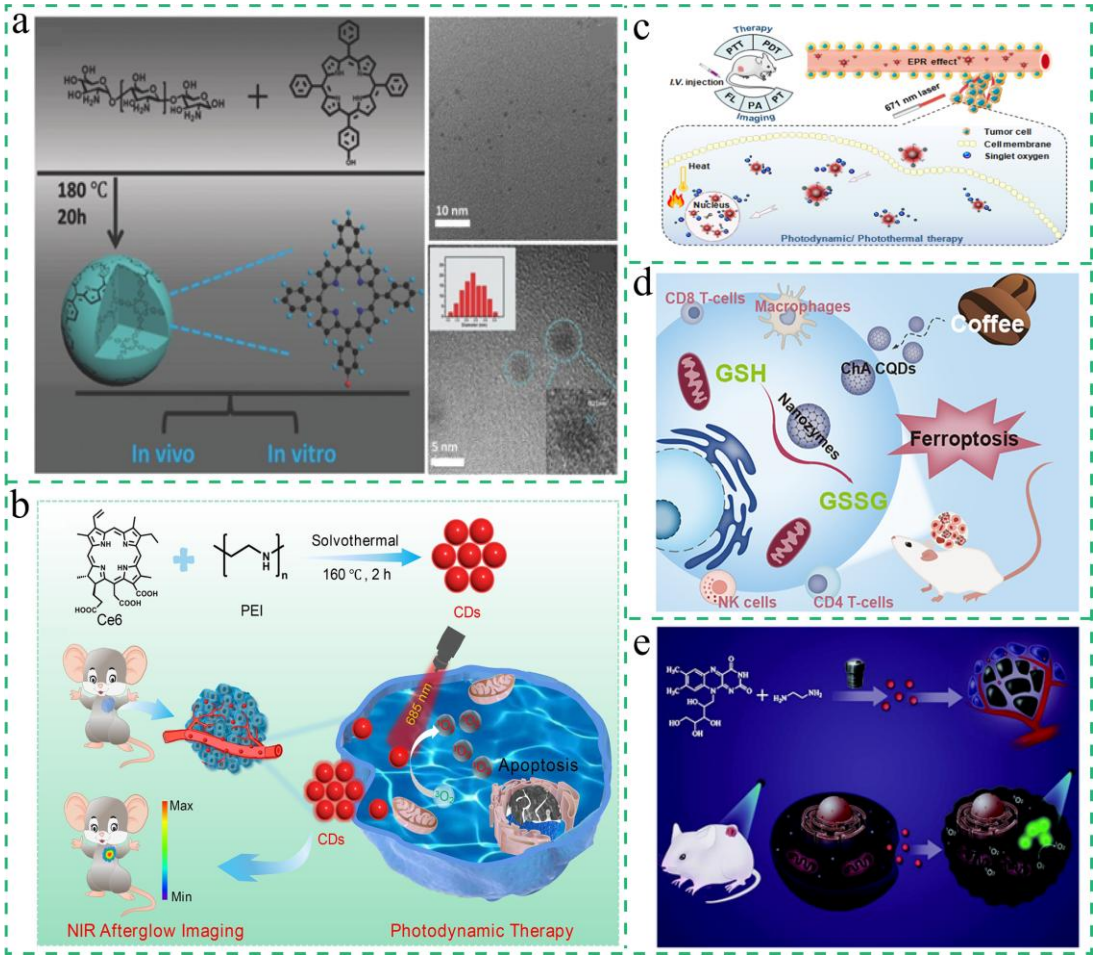

Fig. 4. Applications of CDs in the treatment of cancer. (a) Synthetic route, and characterization images of TPP derived CDs. Reproduced with permission from ref [14]. Copyright 2023 Wiley-VCH. (b) Preparation and procedures of RCDs for afterglow imaging and PDT. Reproduced with permission from ref [63]. Copyright 2023 Elsevier. (c) PDT and PTT synergistic cancer therapy CDs. Reproduced with permission from ref [64]. Copyright 2023 Wiley-VCH. (d) CDs as nanozymes to induce Ferroptosis for cancer treatment. Reproduced with permission from ref [32]. Copyright 2022 American Chemical Society. (e) Natural vitamin riboflavin as a photosensitizer for the treatment of cancer. Reproduced with permission from ref [65]. Copyright 2021 The Royal Society of Chemistry.

In the treatment of disease, drug delivery is as important as the choice of drug. The development of suitable drug delivery systems could facilitate the precise treatment of diseases. In order to be considered an excellent carrier, a substance must meet the following contents. Firstly, the carrier must be capable of targeting a specific lesion. Secondly, the carrier should demonstrate good stability, resist damage from

complex systems and exhibit the capacity to stably bind to the drug, thus protecting it from dissolution or destruction before reaching the target. Finally, the carrier must be able to release the drug once it has delivered drug to a specific site. A number of different nanocarriers have been reported in literature, including silicon nanocarriers, organic nanocarriers, polymer nanocarriers, gold nanocarriers, silver nanocarriers and liposomes. Among them, CDs represents a novel type of drug delivery nanocarriers, which was considered to be excellent drug carriers due to their large specific surface area, better stability and optical stability, low cytotoxicity and easy of modification [66].

Doxorubicin (DOX) is a potent and widely used chemotherapeutic agent that kills rapidly dividing cell, making it a valuable tool in the treatment of malignant tumors. Nevertheless, due to its indiscriminate, dose-dependent, poor solubility and low bioavailability to normal cell, there are some limitations to its use. Therefore, transporting DOX to the target site via a suitable carrier is an effective strategy to reduce its side effects. Yu et al. combined polyethyleneimine passivated CDs with DOX via electrostatic interaction (Fig. 5a). The great water solubility of the CDs increased the uptake of DOX, thereby enhancing the toxicity to HepG2 cell. The results demonstrated that the degree of tumor shrinkage and the survival rate of HepG2 following the injection of the complex was significantly superior to that of DOX alone [67]. Although the aforementioned work has reduced the toxicity of DOX, the undifferentiated toxicity remains detrimental to the patient's health. Therefore, it is

crucial to develop a suitable targeted release for cancer therapy.

Currently, the design of drug carriers based on the differential pH of cancer cell and normal cell is a commonly used method for targeted drug delivery [68-71]. The Warburg effect results in cancer cell being situated in an acidic environment. Therefore, selecting carriers that have a strong ability to release drugs in an acidic environment and a weak ability to release drugs in a neutral or alkaline environment is an effective method of reducing the damage to normal cell. Gong et al. prepared a CDs as a drug carrier using a simple mixture of glucose, ethylenediamine and concentrated phosphoric acid (Fig. 5b). The phosphate group on the surface of the CDs is capable of binding to the protonated amine group on DOX through electrostatic force and hydrogen bonding with a drug loading capacity of 34.53%. At pH 5.0, 96.00% of the drug was released, whereas at pH 7.4, only 24.00% of the drug was released. This significantly reduced the toxicity of DOX to normal cell and enhanced the killing of cancer cell [68]. In addition to the controlled release achieved through the pH responsiveness of the carrier itself, controlled release can also be achieved by controlling the reaction between the carrier and the drug. Yang et al. proposed a nano-delivery system based on DOX and nuclear-localized signal peptide-modified CDs, in which DOX was linked to NLS-modified CDs via an acidic, unstable acylhydrazone bond. The NLS ensured the nuclear targeting function of the CDs, while the acylhydrazone bond cleavage enabled drug release in cancer cell under acidic conditions. *In vivo*, the antitumor activity of DOX-CDs (60.90%) was

higher than that of free DOX (41.60%), and it is expected to be a potential candidate for nuclear targeted drug delivery system (Fig. 5d) [72]. Overall, CDs are promising carriers of anticancer drugs, which is inherently low in toxicity, highly stable and has good tissue permeability, exhibits broad application prospects through the design of rational release and targeting strategies as well as activation. The efficacy of drug carriers for CDs has been extensively investigated, yet challenges remain regarding the specificity of their interaction with tumors and the extension of drug binding and release strategies.

The release of drug can also be controlled by the process of adsorption and desorption occurring between the gel and drug. Wang et al developed a composite ocular drug delivery system by encapsulating CDs in a thermosensitive in situ gel of poloxamer 407 and poloxamer 188 via solubilization loading. This system is designed to enhance the retention time by reinforcing adhesion to the cornea with the gel [73]. Hou et al. developed a nanotherapeutic drug based on honeycomb nano-assemblies of CDs for the sequential and spatiotemporal release of multiple therapeutic agents. The nano-assemblies are capable of accumulating in stroma-rich tumors in vivo through the enhanced permeability and retention effects. Upon dissociation into individual nano-assemblies, the transported losartan and Fe penetrate deeply into the tumor, thereby triggering an enhanced immune response and enabling spatiotemporal release of the drugs [74].

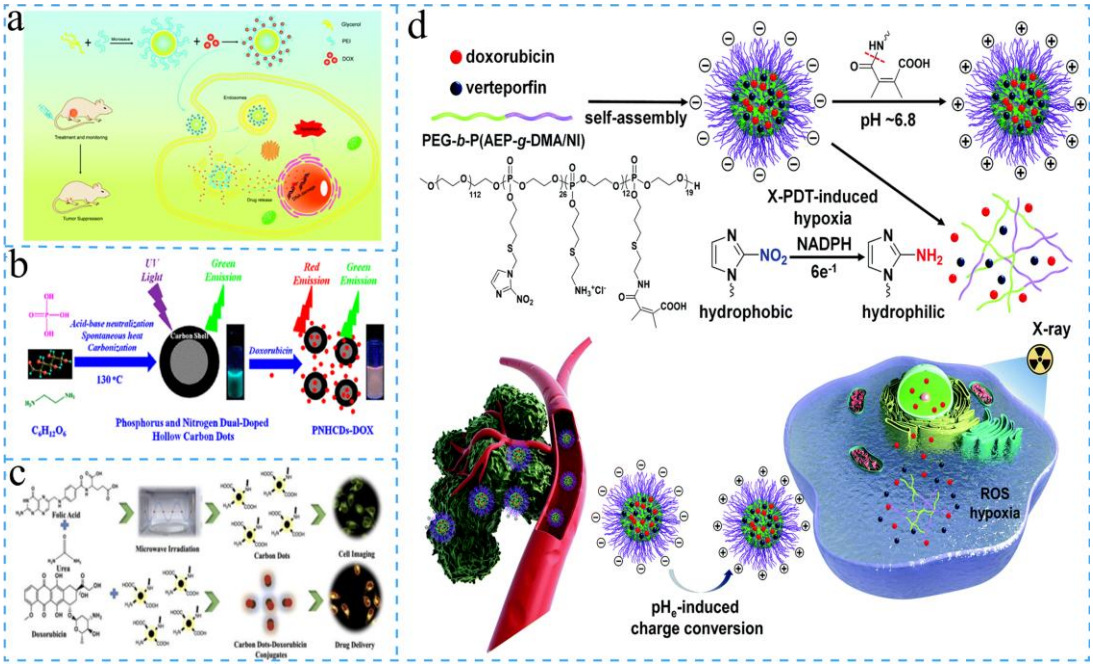

Fig. 5. (a) CD-PEI-DOX used for cancer cell imaging and drug delivery. Reproduced with permission from ref [67]. Copyright 2020 The Royal Society of Chemistry. (b) Ratiometric fluorescence monitoring of CDs for drug release via pH control. Reproduced with permission from ref [68]. Copyright 2016 American Chemical Society. (c) CDs for drug release via pH control. Reproduced with permission from ref [71]. Copyright 2022 Wiley-VCH. (d) CDs for drug release via pH control. Reproduced with permission from ref [72]. Copyright 2020 The Royal Society of Chemistry.

4.2. Applications of CDs in the Treatment of Neurological Disorders

Brain tumors were classified as either primary or metastatic, which can be removed by surgical resection and targeted drug delivery. The best treatment is complete surgical resection; however, this is challenging to achieve due to the precise structure of the brain. Targeted drug delivery can reduce damage to brain tissue and allow precise treatment of brain tumors. However, the targeted drug delivery to the brain places special demands on the delivery vehicle, which must cross the BBB in addition to the most basic carrier requirements. The BBB is a unique and complex multicellular structural barrier in the CNS, consisting of highly semipermeable endothelial cell membranes that allow only oxygen, carbon dioxide, water and small

501 molecules to pass through, while restricting the entry of pathogens and most
502 macromolecules into the CNS. In recent years, the use of NPs in drug delivery has
503 demonstrated many unprecedented properties due to their ability to cross the BBB
504 non-invasively for the treatment of CNS disorders. Among these, CDs exhibit better
505 biocompatibility, lower cytotoxicity and good optical properties to minimize damage
506 to brain tissue [13, 75].

507 CDs have the potential to be employed as a pharmacological agent for the
508 management of CNS disorders. Zhang et al. synthesized CDs with anti-inflammatory
509 and BBB-penetrating ability under alkaline conditions using aspirin as a precursor,
510 which have good fluorescence characteristics and maintain the biological activity of
511 aspirin precursor (Fig. 6a). In both mouse and zebrafish models, significant
512 fluorescence was observed in the brain, indicating that the synthesized CDs retained
513 the ability of aspirin to cross the BBB and also possessed the desirable fluorescence
514 properties of CDs nanoparticles, which is useful for imaging [76]. Cilingir et al.
515 synthesized low-toxicity and good biocompatible CDs using metformin as a precursor,
516 which was localized to mitochondria in cancer cell, but not in normal cell. It was
517 found that the CDs could effectively cross the BBB without the assistance of ligands,
518 and had abundant functional groups on the surface that could be coupled to drugs to
519 enhance therapeutic efficacy (Fig. 6b) [77].

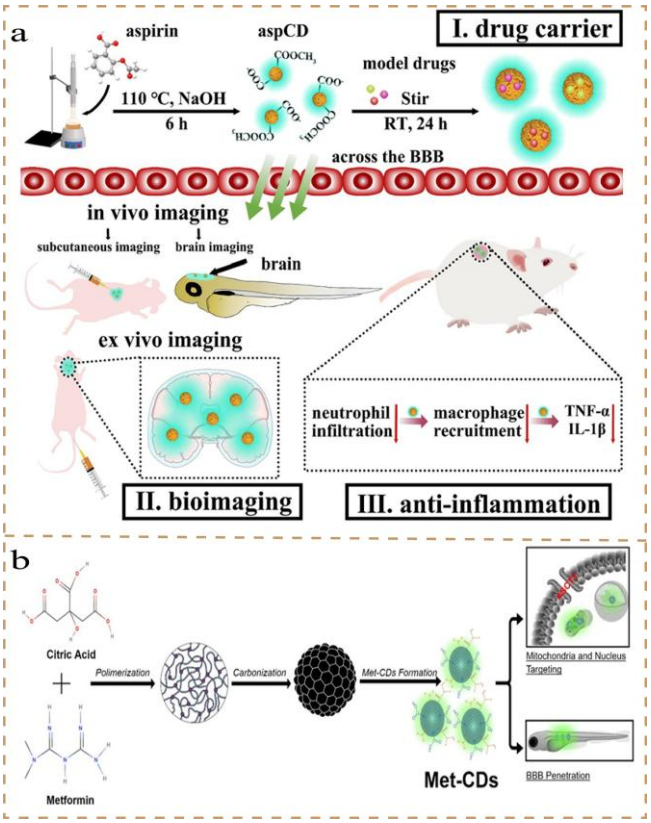

Fig. 6. (a) Synthesis of aspirin derived CDs and its application in the imaging of brain. Reproduced with permission from ref [76]. Copyright 2022 Elsevier. (b) Synthesis of the Met-CDs and its application in the imaging of brain. Reproduced with permission from ref [77]. Copyright 2021 Elsevier.

The initial method for BBB crossing of CDs entailed the linkage of human transferrin-labelled fluorescent dyes to CDs. In 2016, Li et al. prepared CDs from carbon powder, which lacked the ability to cross the BBB to reach the CNS. Upon binding of the CDs to fluorescently labelled human transferrin, bright fluorescence was observed in the CNS of zebrafish. The results demonstrate that CDs can cross the BBB into the CNS, which is the first study of CDs crossing the BBB (Fig. 7a) [78]. This method of transporting CDs by proteins was innovative but failed to achieve treatment for CNS diseases. Researchers subsequently considered loading drugs onto CDs and then attaching human transferrin for targeted drug delivery. Hettiarachchi et al. developed a triple-coupled system for the treatment of brain tumors by coupling

CDs, transferrin, and two anticancer drugs (Fig. 7b) [79]. The average diameter of this system is only 3.5 nm, which facilitates the passage through the BBB for the effective treatment of brain tumors. In this sensing platform, the CDs act as carriers is inherently less toxic. Furthermore, it possesses fluorescent properties that allow for the observation of the drug transport location. Transferrin, on the other hand, increases the cellular uptake of the CDs drug coupler, thus enhancing the anticancer activity.

As the research progressed, it was found that CDs was able to cross the BBB without the presence of transferrin. Zheng et al. synthesized CDs capable of targeting the brain tumor glioma using glucose and aspartic acid as raw materials, with a survival rate of more than 75.0% for both cancer and normal cell at a concentration of 0.5 mg/mL (Fig. 7c) [80]. Furthermore, the endocytosis rate of CDs by cancer cell (72.5%) is significantly higher than that of normal cell (34%), indicating that a comparison between cancer and normal cell toxicity revealed a difference that could be exploited for selective killing of cancer cell. In vivo imaging showed that the CDs accumulated in the mouse brain within five minutes of intravenous injection and was localized in the brain tumor glioma. In conclusion, this work presents a novel approach to the development of vectors that can cross the BBB and shows that CDs lacks transferrin labelling can also cross the BBB and can be employed for the rational drug loading of brain tumor.

CDs has also been used as a carrier to transport drugs for the treatment of

Alzheimer's disease (AD), a progressive neurodegenerative disorder characterized by insidious progression, in which patients present with memory impairment, amnesia, aphasia, dysarthria, cognitive deficits, impaired visuospatial abilities, executive dysfunction, and personality and behavioral changes. The number of treatments for Alzheimer's disease (AD) is limited, primarily due to the low permeability of the BBB to non-steroidal anti-inflammatory drugs (NSAIDs), phenylserine, statins, tafluprednine, ginkgo biloba, trimethoprim and saleptin. However, the use of a carrier to deliver drugs into the CNS represents an effective strategy for treating AD [81-83]. Liu et al. combined graphene quantum dots (GQDs) and ammonium bromide, an inhibitor of β-amyloid aggregation, which improved the ability of ammonium bromide to cross the BBB (Fig. 7d) [83]. The inhibition of β-amyloid aggregation was based on the formation of additional binding sites with Aβ1-42, and the synergistic effect of GQDs and ammonium bromide could better inhibit β-amyloid aggregation, thus providing a new strategy for the exploration of β-amyloid aggregation inhibitor. Using CDs as carriers to deliver photodynamic therapeutic agents to the CNS can improve drug absorption with less harm to patients. Chung et al. prepared red light-excited red CDs that can target β-amyloid. The aptamer-conjugated dots inhibited the self-assembly of Aβ-amyloid under low-injury red light excitation, resulting in a significant β-amyloid aggregation inhibitory effect on β-amyloid aggregation (Fig. 7e). In vivo and in vitro models verified the inhibitory effect of the CDs on β-amyloid aggregation, demonstrating the potential therapeutic effect of this

system in AD [30].

In conclusion, due to their small size, facile surface modification and low toxicity, CDs can be attached to different drugs in different ways and have great potential in brain tumor therapy. However, the self-targeting of CDs to the CNS and the ability to carry drugs into the CNS still require further research, and the mechanism of CDs cross the BBB still needs to be explored. Furthermore, it remains to be determined whether CDs produce toxicity and induce inflammation after entering the CNS.

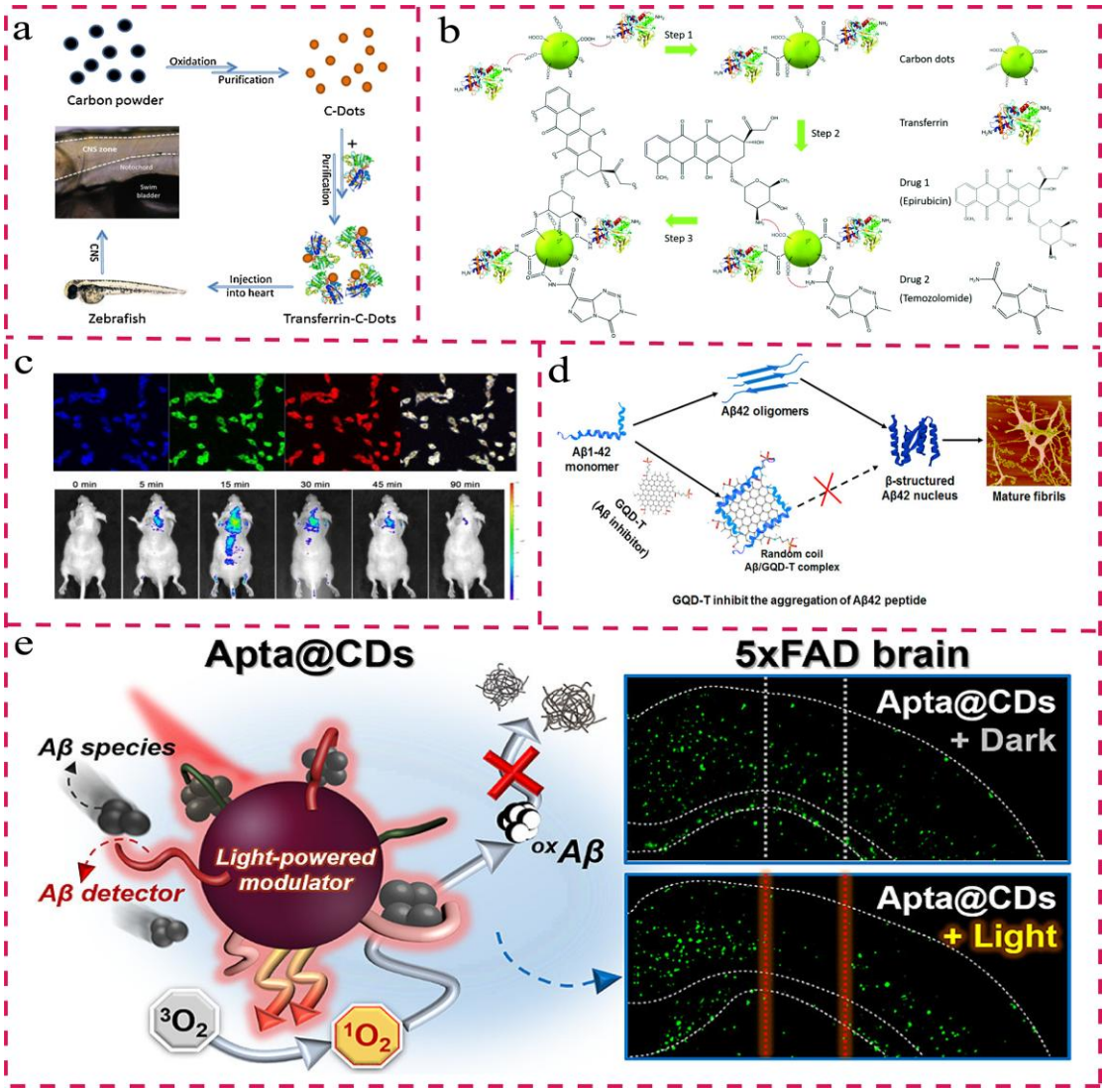

Fig. 7. (a) Transferrin carry CDs crossing BBB of Zebrafish. Reproduced with permission from ref [78]. Copyright 2016 Elsevier. (b) Triple conjugated system composed of transferrin,

4'-Epidoxorubicin and temozolomide on the carboxylic acid functionalized. Reproduced with permission from ref [79]. Copyright 2019 The Royal Society of Chemistry. (c) First CDs crossing BBB without others carrier. Reproduced with permission from ref [80]. Copyright 2015 American Chemical Society. (d) GQDs transport ammonium bromide crossing BBB. Reproduced with permission from ref [83]. Copyright 2018 American Chemical Society. (e) Crossable BBB aptamer-conjugated dots for the treatment of AD. Reproduced with permission from ref [30]. Copyright 2020 American Chemical Society.

4.3. Applications of CDs in antimicrobial

Diseases caused by bacteria are often associated with a high mortality rate and a significant impact on human safety. Currently, antibiotics are employed primarily to treat bacterial infections. However, over time, bacteria have developed resistance to antibiotics, even leading to the emergence of superbugs. Researches have shown that drug-resistant bacteria and common bacteria have similar clinical symptoms, making it difficult to distinguish between them. The continued use of antibiotics has little effect on drug-resistant bacterial infections. Consequently, there is a need to be able to distinguish between these two types of bacteria and prevent the emergence of drug-resistant bacteria. Researchers have found that CDs have good antibacterial effect, not only be used as a photodynamic therapy drug to completely kill bacteria, but also bring antibacterial drugs to the target point to achieve precise antibacterial and reduce the side effects and abuse of drugs, which exhibit a broad prospect of application in antibacterial.

According to previous literatures, the antimicrobial efficacy of CDs is highly related to the positive and negative properties of the groups carried on their surfaces [12, 16, 84]. Since most of the bacterial surfaces are negatively charged, it is necessary to synthesize CDs with positively charged groups on their surfaces for

612 binding to the bacterial surfaces and ultimately inhibiting the bacteria. Qu et al.
613 designed and synthesized positively charged CDs using p-phenylenediamine and
614 polyethyleneimine as precursors, and performed in vitro cytotoxicity, in vivo toxicity
615 and hemolysis tests to demonstrate their good biocompatibility (Fig. 8a). The surface
616 of bacteria is negatively charged, which allows positively charged CDs to bind to the
617 bacterial surface electrostatically, generating a strong electrostatic force that disrupts
618 the bacterial membrane, leading to the death of the bacteria [12]. Furthermore, CDs
619 can scavenge free radicals and possess antioxidant properties that can prevent
620 oxidative stress and promote wound healing in mice. Cheng et al. prepared H-CDs via
621 a straightforward amide condensation reaction using heme chloride and amino-rich
622 CDs as precursors (Fig. 8b). Using an artificial wound mouse model, Staphylococcus
623 aureus was allowed to proliferate in the wound and then the wound was treated with
624 H-CDs. The results showed that the wound healing rate reached 92.80% with the use
625 of H-CDs and laser irradiation. And it was found that the number of colonies was
626 found to be significantly reduced in the presence of H-CDs and laser treatment,
627 indicating that the combination of H-CDs and laser irradiation not only promotes
628 wound healing but also has an antimicrobial effect [16].

629 In addition to CDs that kill bacteria by binding the positive charge on their
630 surface to the negative charge on their surface, a series of CDs that release ROS to kill
631 bacteria have been prepared [14, 31, 85, 86]. Chen et al. prepared N-CDs by the
632 hydrothermal method using lemon peel powder as a precursor. Subsequently, they

prepared nanocomposite membranes by the solvent casting method using the synthesized CDs and chitosan as raw materials (Fig. 8c). The antimicrobial properties were evaluated using the gram-negative bacterium Escherichia coli and the gram-positive bacterium Staphylococcus aureus. The results showed that N-CDs exhibited good antimicrobial properties. In the presence of both light and the composite film (7.00% N-CDs), the bacterial inhibition rate reached 99.99%. This was thought to be due to the release of ROS and other substances from the composite film under the photocatalytic effect, which caused mechanical damage to the bacteria and ultimately inhibited the growth of the bacteria [85]. Wu et al. synthesized CDs (LCDs) with enhanced antibacterial activity and reduced drug resistance utilizing levofloxacin as a raw material. LCDs exhibits a dual antibacterial mode, on the one hand, it can bind to bacteria through electrostatic interactions to rupture the bacterial membranes and kill them; on the other hand, it can generate ROS to block bacterial growth. In vivo tests have shown that LCDs can eliminate bacteria from infected skin or lung tissue in mice without harming other living organism [86].

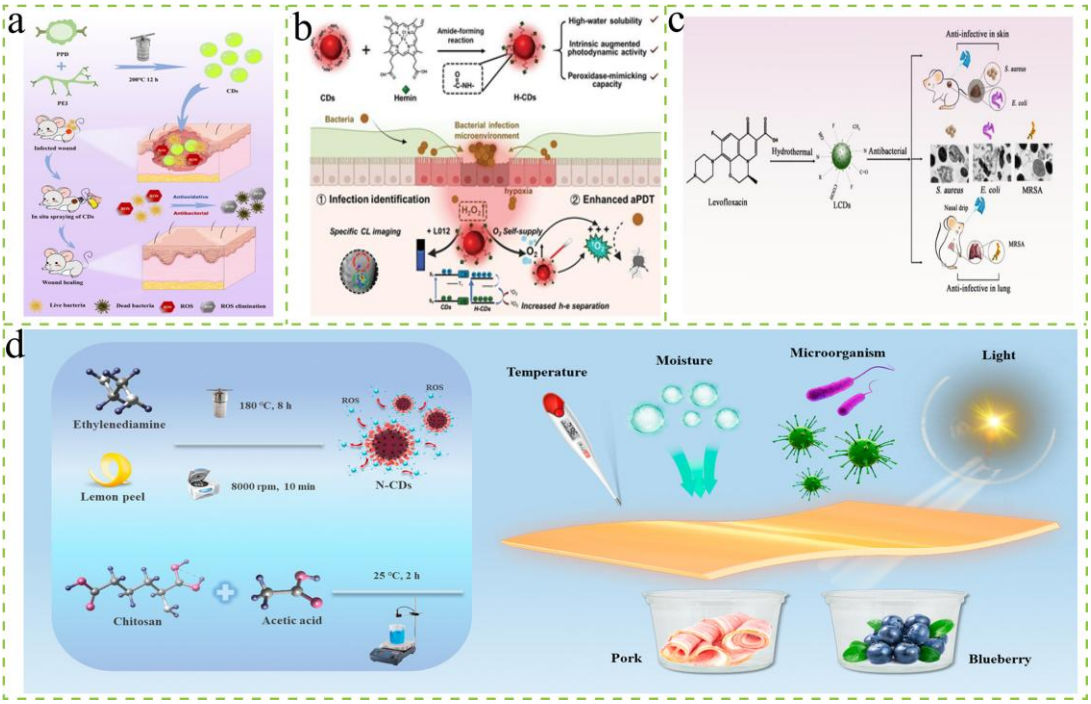

Fig. 8. (a) Synthesis and bacterial therapeutic effects of positively charged CDs. Reproduced with permission from ref [12]. Copyright 2023 American Chemical Society. (b) Preparation of H-CDs and its application for CL imaging and enhanced antimicrobial photodynamic therapy of bacterial infections. Reproduced with permission from ref [16]. Copyright 2023 Wiley-VCH. (c) Preparation of nanocomposite membranes for bacterial therapy. Reproduced with permission from ref [85]. Copyright 2023 Elsevier.

In general, antimicrobial drugs have low water solubility, poor biocompatibility, lack of targeting ability and difficulty in controlling drug release capacity [87]. In 2014, Mukeshchand et al. combined CDs with the antimicrobial drug ciprofloxacin to develop a multifunctional drug delivery system with higher drug capacity exceeding 90.00%. This system was used to deliver a substantial quantity of drug to the bacterial colony (Fig. 9a) [88]. Further investigation revealed that the binding of CDs to ciprofloxacin reduced the toxicity of ciprofloxacin to normal cell, and the drug was released in a controlled manner based on the binding strength of CDs and ciprofloxacin. In the same year, Krishna et al. developed a bone-targeted antimicrobial system by assembling polyethylene glycol-capped CDs with glutamic acid (calcium

665 targeting ligand) and ciprofloxacin (Fig. 9b). The system has minimal cytotoxicity and
666 a haemolysis value of less than 1.00%, which is less harmful to the human body.
667 Based on the above properties and good fluorescence, the system has been used for
668 bone crack detection as well as drug deposition at the crack site for infection control
669 [27].

670 Furthermore, the use of CDs as carriers can enhance permeability of drugs
671 through the cell membrane [79]. Sara et al. improved water-soluble CDs connected to
672 metronidazole in order to enhance the permeability of metronidazole and improve
673 cellular uptake (Fig. 9c) [89]. Metronidazole is an antimicrobial drug for the treatment
674 of periodontal disease, the electron transfer proteins within Porphyromonas gingivalis
675 can reduce the nitro of metronidazole thereby causing loss of bacterial DNA and
676 achieving bactericidal effect. The treatment of periodontal disease is achieved by
677 inhibiting the growth of Porphyromonas gingivalis. However, metronidazole is
678 fat-soluble, which is unfavorable for penetration into eukaryotic cell. After
679 metronidazole is connected with chlorophyll-derived CDs through hydrogen and ester
680 bonding, the chlorophyll-derived CDs can enhance the penetration of metronidazole
681 and make it easier to enter the epithelial cell through the cytoplasm. The drug was
682 taken up by up to 90.00% within three hours, which enhanced the toxicity of the drug
683 against Porphyromonas gingivalis. Moreover, the coupling enhanced the inhibition
684 rate of Porphyromonas gingivalis by 72.00% at the tested concentration, thereby
685 markedly improving the bacteriostatic effect of metronidazole [89].

686 The antimicrobial photodynamic therapy has been developed with the evolution
687 of photodynamic therapeutic approaches, and there is a growing need for integrated
688 therapeutic and diagnostic systems that can facilitate for precision treatment [90, 91].
689 Su et al. developed CDs (Cur-NRCQDs) that integrate diagnostic and therapeutic
690 antimicrobial agents derived from curcumin, which fluoresce up to the near-infrared
691 and have deep tissue penetration, enabling bacterial and cellular imaging and
692 bintegration of bacterial therapy and diagnosis in PDT (Fig. 9d) [90]. In addition, the
693 CDs can be employed as carriers for the transport of curcumin, which improves the
694 storage stability, photostability, ROS generation efficiency and antimicrobial efficacy
695 of curcumin. The authors investigated the antibacterial mechanism of Cur-NRCDs by
696 SEM and CV staining experiments and found that the ROS generated by Cur-NRCDs
697 under light can destroy the phospholipid layer of the bacterial cell membrane and
698 cause the leakage of bacterial inclusions, thus effectively inactivating the bacteria.
699 The combination of CDs with transported commercial antimicrobials can achieve
700 a dual antimicrobial effect through the controlled release of antimicrobials and the
701 generation of synergistic effects [92-94]. Di et al. prepared CDs with high
702 fluorescence QYs, which was combined with the antibiotic Linezolid (LNZ) through
703 hydrogen bonding interactions, resulting in the formation of a composite system of
704 LNZ-CDs (Fig. 9e) [92]. This system with high drug encapsulation and loading rates
705 of 97.2 ± 1.0/22.5 ± 0.23%, and controlled release of LNZ could be achieved, which
706 was completed within 48 hours for the LNZ-CDs system compared to the 6-hour drug

707 release of LNZ only. The release of LNZ reaches a bottleneck in the first 12 hours,
708 followed by a slow release, which achieves a bacteriostatic effect while continuously
709 stimulating the renewal of injured tissues. Moreover, the hemolysis rate of this
710 LNZ-CDs system was of less than 5.00%, which was lower than that of LNZ
711 (14.00%), improving the speed of wound recovery and promoting wound healing.

712 Additionally, CDs can facilitate the simultaneous transport of a commercial
713 photosensitizer and antimicrobial agent, thereby achieving optimal antimicrobial
714 effects. In 2017, Liu et al. designed a multifunctional nanoplatform with a bilayer
715 structure as a carrier loaded with CDs, bengal rose and ampicillin (Fig. 9f) [94]. The
716 mesoporous silica nanoparticles prevented the ACQ of CDs and photosensitizer,
717 where CDs was responsible for the fluorescence imaging, and the combined effect of
718 bengal rose and ampicillin enhanced the antimicrobial effect, which possess higher
719 release rate (1.4-fold) of single-linear oxygen compared to pure oxygen, further
720 enhancing the ability of sterilization.

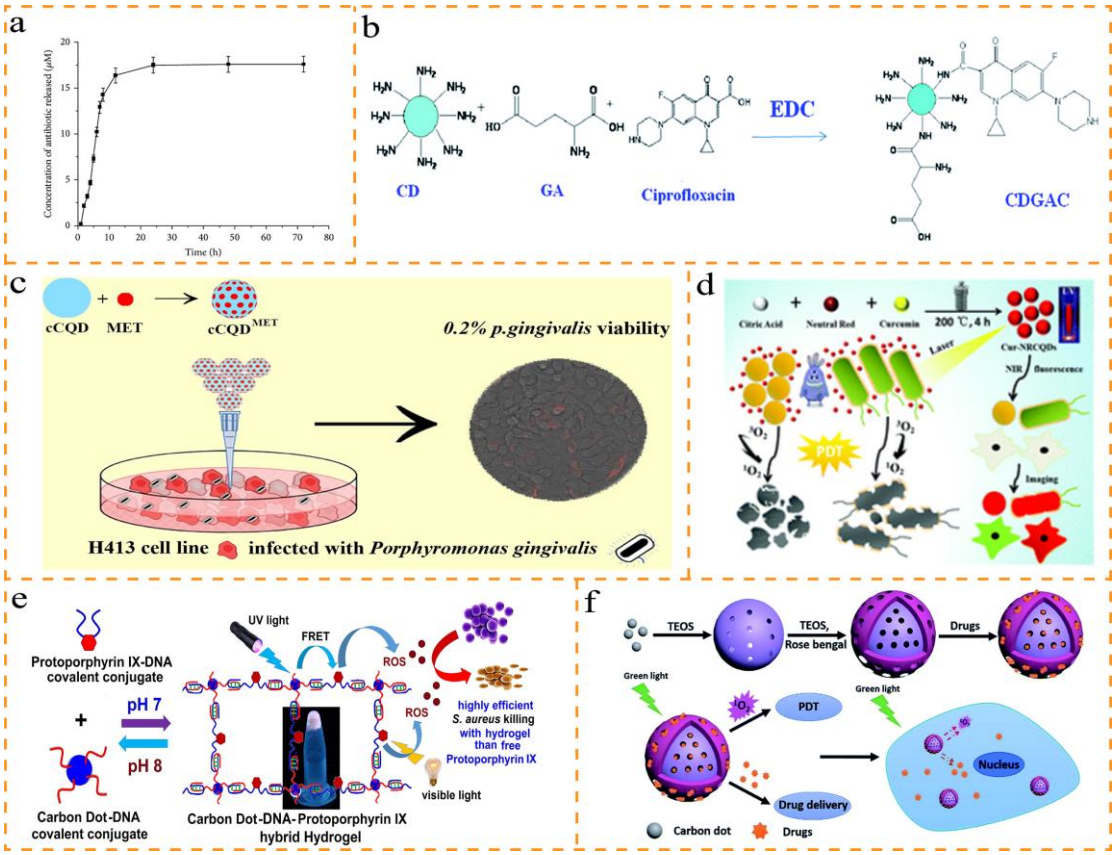

Fig. 9. (a) Time-dependent release profiles of antimicrobial drugs transported by CDs. Reproduced with permission from ref [88]. Copyright 2014 Europe PubMed Central. (b) CDs for bone fracture detection and transport of therapeutic drugs. Reproduced with permission from ref [27]. Copyright 2014 The Royal Society of Chemistry. (c) CDs transport metronidazole for the treatment of periodontitis. Reproduced with permission from ref [89]. Copyright 2019 Elsevier. (d) Schematic diagram of curcumin-derived CDs transporting curcumin to bacteria for diagnostic and therapeutic integration. Reproduced with permission from ref [90]. Copyright 2021 The Royal Society of Chemistry. (e) Hybrid hydrogel of CDs, Protoporphyrin IX (PpIX) and DNA for photodynamic therapy to kill Staphylococcus aureus Reproduced with permission from ref [91]. Copyright 2019 Elsevier. (f) Simultaneous delivery of antimicrobial and photosensitizer for antimicrobial therapy by one CDs. Reproduced with permission from ref [94]. Copyright 2017 The Royal Society of Chemistry.

In addition to loading antimicrobial drugs and photosensitizers, CDs was used to store antimicrobial gases. Liu et al. prepared fluorescent CDs (CPA-CDs) using chitosan-grafted polyamide dendritic polymers as a carbon source, and then loaded NO onto the CDs to form *N*-diazodicarboxylic acid esters (CPA-CDs/NONOate), which showed excellent antibacterial effects with three times of NO content (Fig. 10a)

[95]. And this CDs can image bacteria while simultaneously inhibiting them due to its fluorescence properties. In vivo antimicrobial experiments demonstrated that CPA-CDs/NONOate was an effective sterilizing agent for wounds in experimental mice, and exhibited anti-inflammatory and wound healing properties.

CDs was employed for the capture, characterization and eradication of superbugs (Fig. 10b). Pramanik et al. synthesized blue CDs bind to the activated carboxylated magnetic nanoparticles by amide bonding, then the complex is activated by EDC/NHS and then binds to the Salmonella DT104 antibody which can be used for identification, isolation, detection and complete virulence killing of superbugs. The synthesized red CDs, was used for capture Salmonella MRSA in the same way, and because of the good fluorescence, the isolated bacteria can be fluorescently imaged, allowing identification and characterization of superbugs as well as complete viral killing. In addition, the CDs allowed fluorescent imaging of the isolated bacteria, enabling the identification of Salmonella DT104 and MRSA. In conclusion, this study provides a new material for the capture, characterization and eradication of superbugs, offering a viable solution to superbugs [96].

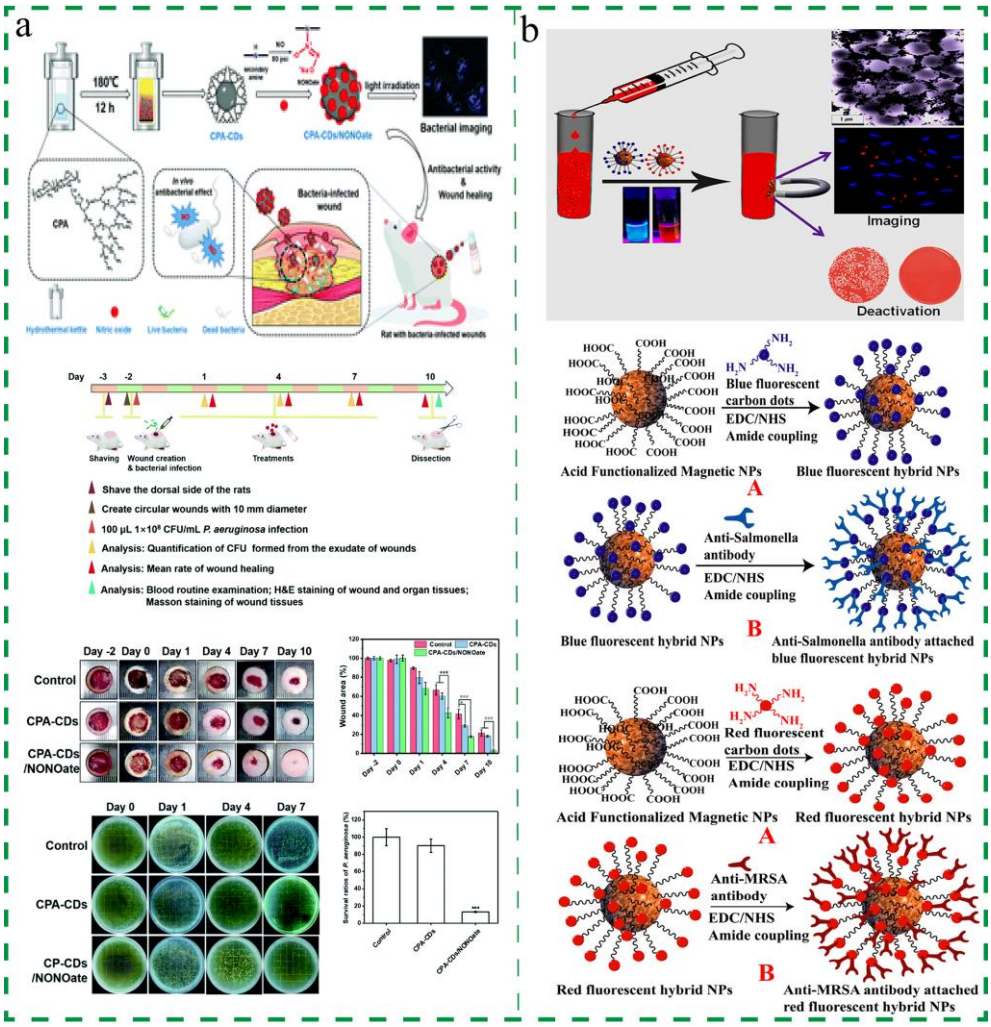

Fig. 10. (a) CDs as carriers to transport antibacterial gas NO for bacterial imaging and therapy. Reproduced with permission from ref [95]. Copyright 2021 The Royal Society of Chemistry. (b) Multifunctional CDs attached to magnetic nanoparticles for isolation and identification of superbugs Reproduced with permission from ref [96]. Copyright 2017 American Chemical Society.

4.4. Applications of CDs in Antiviral

Bacteria can be treated with a variety of antibiotics, but there are no specific therapeutic drugs for viruses. Viruses are composed of nucleic acids and proteins that depend on their host for survival, making them difficult to kill, which can only be achieved by antibodies or vaccines. Viruses have been discovered for a long time, including the smallpox virus and infectious viruses, which have caused great harm to human beings, so it is very meaningful to study antiviral drugs [7]. It has been

768 demonstrated that carbon-based nanomaterials possess the potential to exhibit
769 antiviral properties, thereby providing the desired biocompatibility and antiviral
770 properties. Some CDs have been demonstrated to possess antiviral capabilities,
771 including the release of single linear oxygen species or interference with viral
772 enzymes through photoexcitation, which serve as functional molecular platforms to
773 trap and inhibit viral activity. Furthermore, the delivery of antibodies to the body
774 using CDs has been reported to be an effective method of destroying viruses.
775 Although the field of research into the use of CDs as antiviral agents is not yet fully
776 developed, published results suggest that this area is promising and may contribute to
777 the development of innovative antiviral therapies. Nevertheless, the field of research
778 is evolving in response to the ever-changing viral threat. Further experimental and
779 clinical studies are required to validate these concepts and advance the practical
780 application of antiviral nanomaterials [15].

781 Lin et al. investigated the antiviral effects of curcumin-derived CDs (Cur-CQDs)
782 against Enterovirus 71 (EV71). The results showed that Cur-CQDs exhibited notable
783 antiviral efficacy. During the synthesis, the surface characteristics and activity of
784 curcumin underwent alterations contingent on the heating temperature (Fig. 11a). In
785 vivo experiments showed that the intraperitoneal injection of curcumin CQDs
786 significantly reduced the effects of EV71 virus on newborn mice and protected them
787 from virus-induced hind limb paralysis [97]. Tong et al. synthesized a biocompatible
788 CDs (Gly-CDs) from the active ingredient (glycyrrhizic acid) of a Chinese herb using

a hydrothermal method and investigated its antiviral effects against porcine reproductive and respiratory syndrome virus (PRRSV) [98]. The results showed that Gly-CD effectively inhibited the proliferation of PRRSV and exerted its antiviral effects through a variety of mechanisms, including inhibition of viral invasion and replication, the stimulation of antiviral immune responses, and reduction of intracellular ROS accumulation. In addition, Gly-CDs was also found to have significant antiviral activity against other viruses, such as pseudorabies virus (PRV) and porcine epidemic diarrhea virus (PEDV), suggesting its widely range of antiviral potential. The collective findings indicate that Gly-CDs exhibits remarkable antiviral activity and multisite inhibition mechanisms, rendering it a promising candidate for alternative therapies for PRRSV infection. (Fig. 11b). CDs can achieve virus inactivation by changing the surface protein structure of viruses. Du et al. prepared cationic antiviral CDs from the Chinese herbal medicine curcumin, and the positively charged CDs can cause viral aggregation through electrostatic interactions, thereby reducing viral infectivity (Fig. 11c) [99]. The CDs can alter the surface protein structure of the virus, impede virus entry, reduce the synthesis of viral negative-stranded RNA, and inhibit the accumulation of ROS and viral outgrowth.

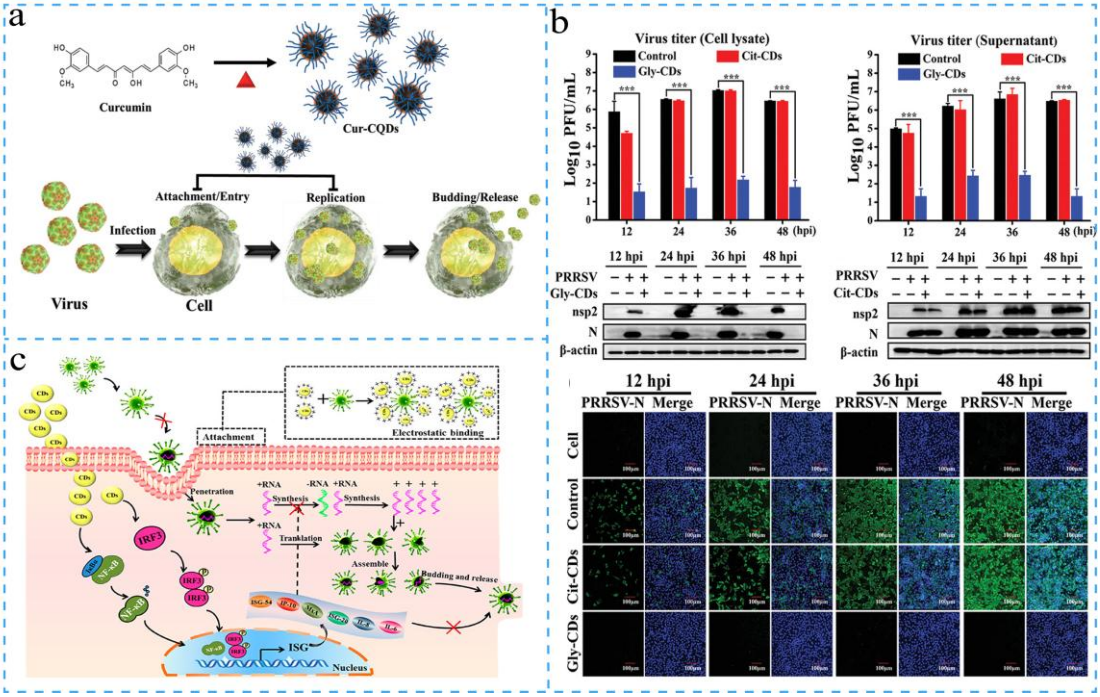

Fig. 11. (a) Preparation of curcumin-derived CDs for use against EV71 virus. Reproduced with permission from ref [97]. Copyright 2019 Wiley-VCH. (b) Gly-CDs for anti-PRRSV. Reproduced with permission from ref [98]. Copyright 2020 Wiley-VCH. (c) Schematic representation of curcumin-derived CDs for anticoronaviral. Reproduced with permission from ref [99]. Copyright 2018 American Chemical Society.

The delivery of appropriate antibodies into the body represents an effective method for the destruction of viruses. Ju et al. used CDs-loaded Locked Nucleic Acid (LNA)-based oligonucleotides to knock down miR-K12-1, miR-K12-4, and miR-K12-11 encoded by Kaposi's sarcoma-associated herpesvirus (KSHV), thereby induced apoptosis and then inhibited the proliferation of primary effusion lymphoma cell (Fig. 12a). The system effectively inhibited the initiation of PEL effectively without significant toxicity to KSHV-negative cell. Moreover, this method displays enhanced specificity and efficiency compared to conventional treatments and induces tumor regression in established PEL mouse models, markedly improving animal survival [100]. Vaccines for avian influenza in chickens have been widely used, and it

822 is important to identify high-quality target antigens to combine with the vector for an
823 effective next-generation vaccine. Cheng et al. extracted and loaded recombinant
824 gp85 protein, an antigen of Avian Leukemia Virus Subgroup J (ALV-J), onto CDs and
825 vaccinated chickens (Fig. 12b). The CDs demonstrated a protective effect against the
826 antibodies, with an antibody detection rate that was 6.3 times higher than that of the
827 unloaded group at 11 weeks. This evidence supports the hypothesis that loading CDs
828 with antibodies confers a benefit [101].

829 Additionally, CDs have been demonstrated to serve as effective anti-HIV carriers,
830 capable of inhibiting the replication of the HIV virus [102]. Iannazzo et al. prepared
831 graphene QDs to load a reverse transcriptase inhibitor through an amidation reaction
832 for the treatment of HIV (Fig. 12c). The RTI-coupled compound, GQD-CHI499,
833 showed an IC50 value of 0.09 μg/mL in cell and EC50 values of 0.066 μg/mL, which
834 is a great improvement compared to either pure CDs or pure drug. The target of action
835 of the drug conjugates GQD-CHI499 and GQD-CDF119 in the HIV replication cycle
836 was also investigated using the Time-of-Addition (TOA) method, which demonstrated
837 inhibition of the HIV virus.

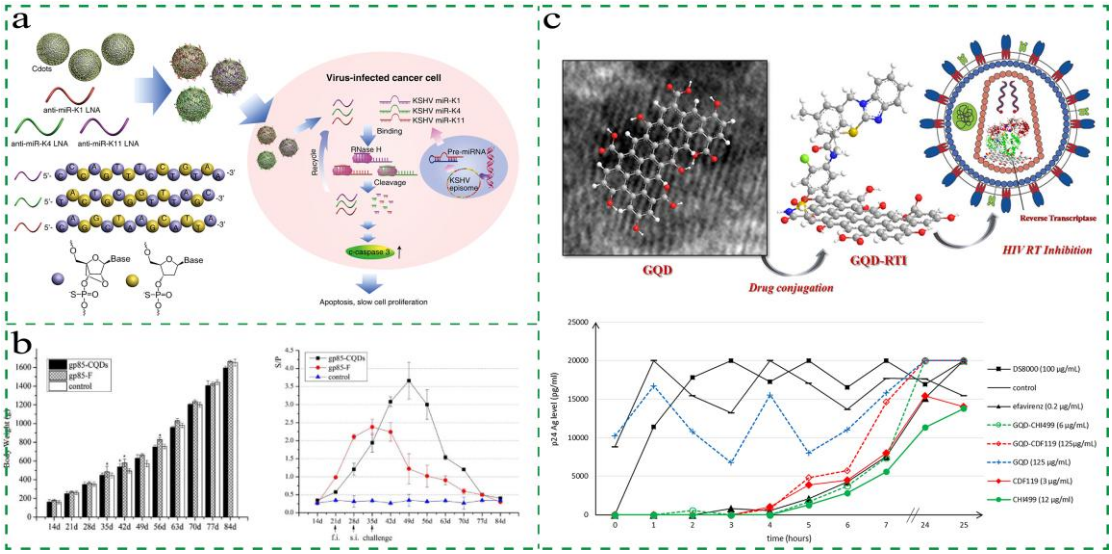

Fig. 12. (a) CDs loaded (LNA-based oligonucleotides to induced apoptosis of KSHV. Reproduced with permission from ref [100]. Copyright 2020 American Chemical Society. (b) Therapeutic efficacy of CDs transported gp85 protein as a new generation of avian influenza vaccine for chickens. Reproduced with permission from ref [101]. Copyright 2019 Elsevier. (c) GQDs based systems as HIV inhibitors. Reproduced with permission from ref [102]. Copyright 2018 American Chemical Society.

Overall, CDs have been employed as drugs and carriers for various drugs due to their high stability, excellent optical properties, good water solubility, and ease of modification, demonstrating their significant potential to enhance drug efficacy by enhancing membrane permeability and absorption of drugs, controlling the release rate and prolonging the in vivo circulation time of drugs, enhancing the ability to cross the BBB. Nevertheless, there are still some issues that require to be solved in the use of CDs as a drug delivery system, such as the controllable preparation of CDs, the toxicity and mechanism of action after crossing the BBB are still unclear, and the ability to maintain the corresponding effect in complex biological systems needs to be studied urgently.

4.5. Applications of CDs in Drug Analysis

The advent of medical technology has led to the resolution of numerous complex

857 medical conditions. However, this has also precipitated the emergence of novel
858 challenges, such as the potential for overdose or mishandling of drugs to yield adverse
859 outcomes. The abuse of drugs not only has irreversible effects on the environment, but
860 also poses serious hazards to the human body. The ingestion of excessive quantities of
861 pharmaceuticals can result in a range of adverse effects, including the development of
862 hypoglycaemia (low blood sugar) and syncope (fainting) due to the excessive use of
863 antihypertensive drugs. The abuse of drugs has a significant impact on the
864 environment and human health globally. Consequently, it makes sense to implement
865 an effective system to monitor drugs in environment.

866 CDs was used to analyze anti-cancer drugs. Zorubicin and DOX are
867 chemotherapeutic drugs for the treatment of cancer, however, which are associated
868 with many side effects. Therefore, monitoring their levels in the human body is
869 meaningful for the patients' physical conditions. Mohammadinejad et al. prepared blue
870 CDs using bell pepper as raw material, then combined them with red CdTe QDs
871 encapsulated in silica to realize the ratiometric detection of anthraquinones (Fig. 13a).
872 The electrostatic interactions between drugs and CDs resulted in the fluorescence
873 quenching of the CDs. Conversely, the surface charge of Si@CdTe can keep it away
874 from Zorubicin and DOX and exhibit stability fluorescence, so as to realize the
875 ratiometric detection of anthraquinone drugs, which has the advantages of low
876 background interference, environmental friendliness, fast response as well as a wide
877 range of response [103]. However, the fluorescence of the CDs is blue, the depth of

878 tissue penetration is low, and the blue light of the biological tissue itself will cause
879 interference Zhong et al. prepared near-infrared-emitting CDs with citric acid and
880 urea as raw materials, which had excitation wavelengths of 560 nm and emission
881 wavelengths of 655 nm, the increased concentration of MITX caused a reduced
882 fluorescence due to the overlap absorption of MITX and CDs and realized the
883 detection of MITX (Fig. 13b) [104].

884 CDs was employed to analyze antimicrobial drugs [3, 101-106]. Norfloxacin, a
885 fluoroquinolone antimicrobial, has been present in surface water, soil, fish and shrimp
886 due to its widespread use, which is potentially a threat to human health. Two CDs for
887 the detection of norfloxacin were prepared from 2,3-diaminonaphthalene and
888 1,8-diaminonaphthalene, respectively (Fig. 13c). Due to the differing size and spectral
889 properties of the two CDs, their sensing modes for norfloxacin were distinct.
890 Norfloxacin binds to the CDs via hydrogen bonding, which enhances the fluorescence
891 of 2,3-CQDs based on the charge transfer between norfloxacin and the CDs, and
892 quenches the fluorescence of 1,8-CQDs based on the resonance energy transfer
893 between norfloxacin and the 1,8-CQDs. The combination of the two CDs enables the
894 accurate detection of norfloxacin and reduces the likelihood of false positives [105].

895 Tetracycline is a commonly used antimicrobial drug that is widely employed to
896 treat bacterial infections. However, excessive tetracycline use may be harmful to
897 human body, which has attracted considerable attention with regard to the detection of
898 tetracycline. Wang et al. constructed a fluorescent sensor based on fluorescent CDs

899 embedded in MOF and combined with molecular blotting technology for the detection
900 of tetracycline (Fig. 13d). The CDs was used as fluorophores, and porous ZIF-8 was
901 used as a support carrier to improve the adsorption capacity of the complex, then the
902 MOF-supported molecularly imprinted CDs was prepared by a Sol-gel strategy, and
903 realized the detection of tetracycline in milk and eggs based on the internal filtration
904 effect of tetracycline on this material [106].Wang et al. prepared a blue CDs for the
905 detection of azithromycin by hydrothermal method using dried beetroot powder as
906 raw material (Fig. 13f). The CDs is oil-soluble and weakly fluoresces in water due to
907 ACQ, while azithromycin can bind to the hydroxyl group on the surface of the CDs,
908 thus reducing the aggregation of CDs and achieving the turn-on detection of
909 azithromycin [107]. Additionally, RTP CDs have been employed for the detection of
910 antimicrobial drugs [108, 109]. Wang et al. prepared CDs to detect metronidazole in
911 both fluorescence and phosphorescence modes. It was observed that metronidazole
912 can quench the fluorescence and phosphorescence of CDs through the internal
913 filtration effect, thereby enabling phosphorescence detection [108].

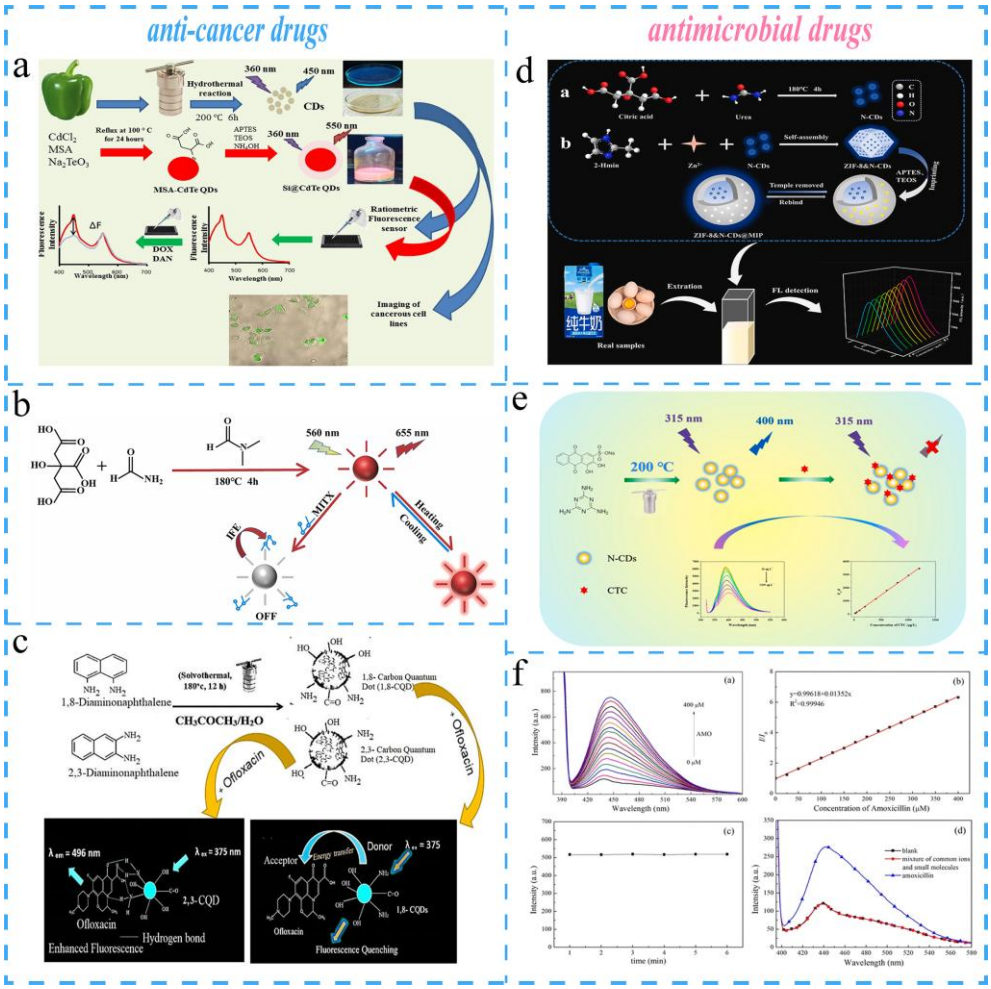

Fig. 13. (a) CDs prepared from bell peppers for the detection of DOX. Reproduced with permission from ref [103]. Copyright 2023 Elsevier. (b) NIR CDs detection of MITX prepared from citric acid. Reproduced with permission from ref [104]. Copyright 2023 Elsevier. (c) Schematic representation of the preparation and response mechanism of two CDs for the detection of norfloxacin. Reproduced with permission from ref [105]. Copyright 2023 Elsevier. (d) Detection of tetracycline by CDs-conjugated molecular blotting technique. Reproduced with permission from ref [106]. Copyright 2018 Elsevier. (e) CDs for the detection of chlortetracycline Reproduced with permission from ref [110]. Copyright 2024 Elsevier. (f) CDs prepared from beetroot for the detection of azithromycin. Reproduced with permission from ref [107]. Copyright 2018 Springer.

CDs was used to analyze antiviral drugs [111-113]. Hepatitis B virus (HBV) infection slightly increases the risk of liver disease, but the current methods for detecting hepatitis B virus suffer from low sensitivity, time-consuming, etc. Guo et al. constructed an electrochemiluminescence (ECL) biosensor using CDs as the luminescent agent by combining a ternary ECL system and a target DNA

amplification strategy (Fig. 14a). First, boron and nitrogen co-doped CDs was prepared with citric acid, urea, boric acid and modified on the electrode, then a quenching group was attached to quench its ECL by capturing DNA when the target viral DNA (HBV-DNA) appeared, the initiating group could be left by cyclic amplification, and the ECL was enhanced, which could achieve the turn-on detection of HBV-DNA. The method is highly sensitive with a LOD of 18.08 aM and a detection range of 100.00 aM-1.00 nM, providing a new strategy for clinical hepatitis B virus detection [111].

CDs-based sensing platforms had also been used to analyze foodborne toxins and pathogenic bacteria, Wang et al. covalently doped CDs into mesoporous nanoparticles (CDs-MSNs) for flow measurement immunoassays (Fig. 14b). They constructed sensing test strips for the detection of aflatoxin B1 and Staphylococcus aureus based on both competitive and sandwich models, with LOD as low as 0.05 ng/mL and 102.00 cfu/mL, respectively. The use of CD-MSN for the detection of aflatoxin B1 and Staphylococcus aureus in foodstuffs provides a new idea for the detection of other similar viruses [113]. Novel coronaviruses are responsible for the largest health and safety incidents in recent years, and rapid detection of novel coronaviruses is important for virus prevention. Xu et al. prepared blue CDs by hydrothermal method, and the carboxylated CDs emitting red fluorescence were obtained by treatment with sodium hydroxide and hydrochloric acid. Then *N*-β-(aminoethyl)-γ-aminopropyltrimethoxysulfonate (AEAPTMS) conjugated to

silica carrier was grafted onto silica carrier by amidation reaction, which were then coated with 3-aminopropy triethoxysilane (APTES) to obtain SiO2@CD@SiO2 spheres (Fig. 14c). AEAPTMS was grafted onto the silica carrier by amidation reaction to obtain silanized silica carrier, which was then capped with APTES to obtain SiO2@CD@SiO2 spheres.SARS-CoV-2 nuclear head protein (SARS-CoV-2NP) was then modified on the SiO2@CD@SiO2 beads, and the detection of newly conjugated viruses was achieved by the antibody-antigen reaction, with a detection sensitivity of 100.00 pg/mL under UV light, which can be designed as a rapid kit for detection of new coronaviruses in blood [114].

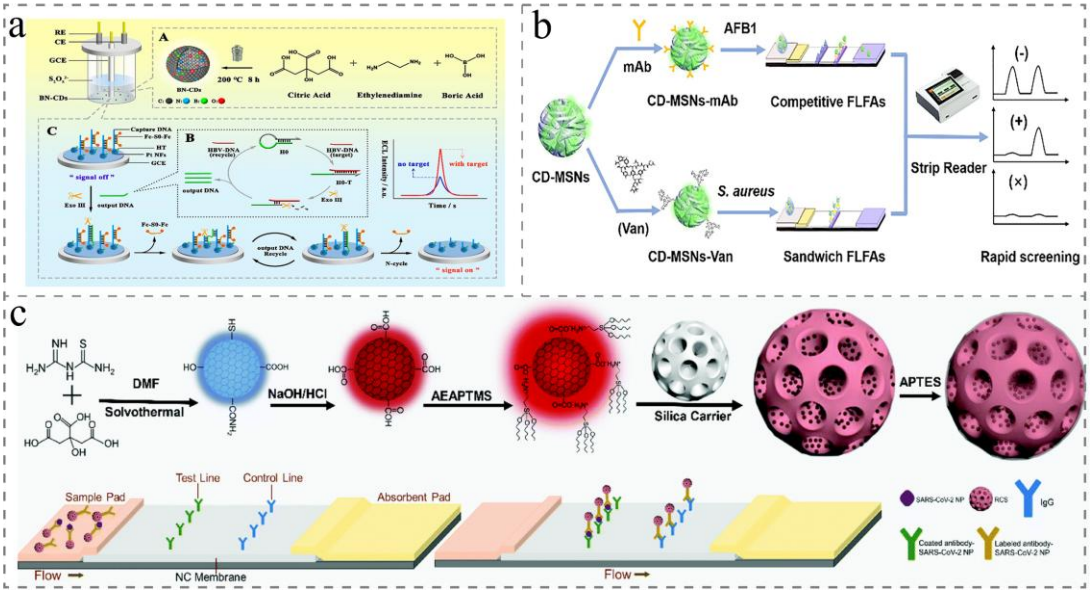

Fig. 14. (a) CDs-based ECL biosensor for HBV detection. Reproduced with permission from ref [111]. (b) CDs doped inside mesoporous nanoparticles for the detection of foodborne toxins and pathogenic bacteria. Reproduced with permission from ref [113]. Copyright 2023 Elsevier. (c) Hydrothermal preparation of CDs for the detection of new coronaviruses. Reproduced with permission from ref [114]. Copyright 2021 Elsevier.

CDs was used to analyze pesticides [115]. Organophosphorus pesticides (OPs) can inhibit acetylcholinesterase, which is an important enzyme in the human body and involved in the processes of oxidative stress, apoptosis, inflammation, and

969 tumorigenesis, so monitoring the concentration of OPs is of great significance [23].
970 Lan et al. prepared green luminescent CDs that emitted green fluorescence under
971 excitation light at 410 nm (Fig. 15a). The drug methyl parathion is converted to
972 p-nitrophenol under alkaline conditions, which has a strong absorption peak at 403
973 nm, therefore the green fluorescence of the CDs was quenched by the internal
974 filtration effect, which realized the detection of methyl parathion. However, turn-off
975 detection is easily disturbed by the complex environment, and it is easy to have false
976 positives [116].

977 The inhibition of acetylcholinesterase activity by OPs is a commonly used
978 method for the detection of OPs. Lin et al. achieved turn-on detection of fluorescence
979 based on the inhibition of acetylcholinesterase activity by OPs, which inhibited H_2O_2
980 production and the catalysis of Fe^{3+} by Fe^{2+} (Fig. 15b) [117]. Li et al. prepared red
981 fluorescent CDs and constructed a sensor platform for the ultrasensitive detection of
982 OPs (Fig. 15c). Dopamine attached to the CDs can quench the red fluorescence of the
983 CDs while emitting green fluorescence at 503 nm, while acetylcholinesterase can
984 inhibit aggregation of dopamine, thus quenching its green fluorescence and enhancing
985 the red fluorescence. OPs can inhibit the activity of acetylcholinesterase, which can
986 enhance the green fluorescence and quench the red fluorescence, thus achieving
987 ultra-sensitive detection of OPs with a LOD of 0.025 ng/mL [118]. The detection of
988 OPs can also be realized through the oxidation of OPs on metals. Hiremath et al.
989 constructed a sensing platform for the detection of hydrazine using blue CDs prepared

990 from potato pulp and immobilized CDs on manganese nanosheets to burst the
991 fluorescence of the CDs via Förster resonance energy transfer (FRET), whereas
992 hydrazine reduces MnO_2 to Mn^{2+}, releasing the CDs to enhance the fluorescence,
993 enabling the detection of hydrazine and providing a simple solution for the detection
994 of hydrazine in pesticide prodrugs (Fig. 15d). It is a simple solution for the detection
995 of hydrazine in pesticide prodrugs [119]. Paraquat is a rapidly inactivating herbicide
996 with touch kill and certain systemic effects, so it is widely used for weeding, but
997 paraquat is highly toxic to human body and there is no specific therapeutic drug, so
998 the detection of this pesticide residue is of great significance to the safety of human
999 lives.

1000 Chen et al. prepared blue luminescent CDs and red luminescent copper
1001 nanoclusters with AIE properties and combined them by electrostatic interaction to
1002 construct a sensing platform that can differentially detect fumonisin and paraquat (Fig.
1003 15e). The complex has negative electronegativity, and at a water content of 5.00%, the
1004 S-S bond of thiram binds to Cu^{2+}, causing its red fluorescence to burst, which
1005 achieves ratiometric detection of fumonisin; while at 100.00% water content, due to
1006 the effect of AIE, the blue fluorescence bursts and the red fluorescence appears, and
1007 the positively charged water-soluble paraquat binds to the complex, facilitating
1008 ratiometric detection of paraquat [120].

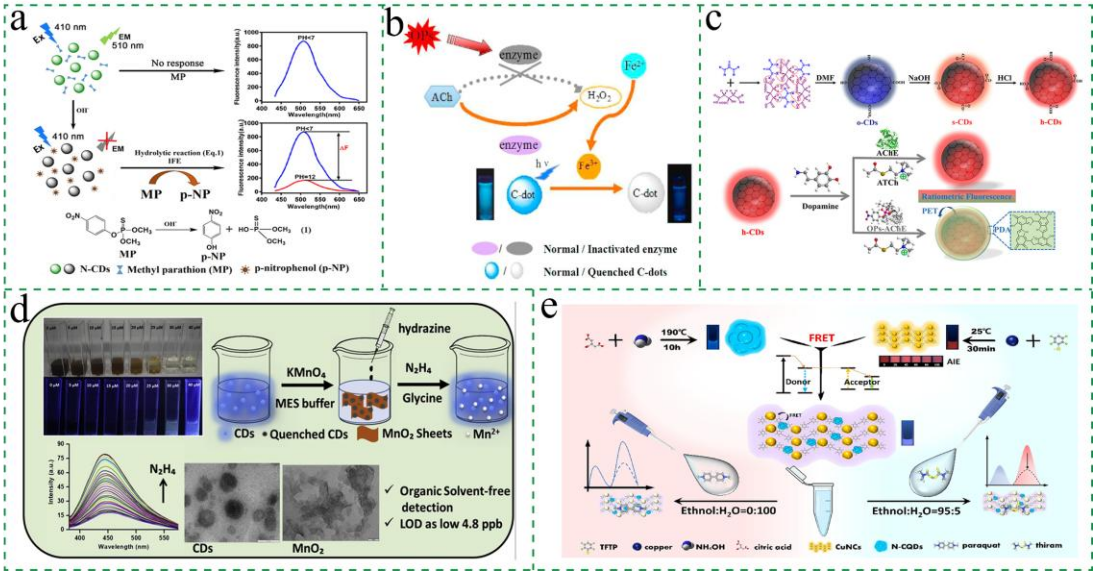

Fig. 15. (a) Illustration of IFE-based fluorescent sensor for methyl parathion using CDs. Reproduced with permission from ref [116]. Copyright 2019 Elsevier. (b) Mechanism for the detection of organophosphorus pesticides by unmodified CDs. Reproduced with permission from ref [117]. Copyright 2018 Elsevier. (c) Synthesis route of h-CDs and its mechanism for detecting OPs. Reproduced with permission from ref [118]. Copyright 2020 American Chemical Society. (d) Preparation and application of CDs for the detection of hydrazine based on the redox reaction of MnO_2 and hydrazine. Reproduced with permission from ref [119]. Copyright 2020 Elsevier. (e) Combined blue AIE CDs and red ACE copper nanoclusters for ratio detection of paraquat. Reproduced with permission from ref [120]. Copyright 2022 Elsevier.

CDs was used to analyze other drugs. Some criminals often add drugs to the victims' drink, as the previous analysis methods all need long time and complicated means, it is difficult to detect this drug quickly due to its strong hidden nature. Yen et al. used hydrophobic CDs as fluorophore, dissolved it in 0.50 mL of toluene, the nitro-substituted benzodiazepines and nimetazepam in the drink will happen electron transfer with CDs (Fig. 16a). This quenched the fluorescence of the CDs and the detection limit was 7.24 μM, well below the detection concentration at most crime scenes[121]. Drugs containing thiol groups play an important role in the human body, and the current methods for detecting such drugs are both complex and expensive. Mehta et al. prepared core-shell nanomaterials (Au-CQDs) by combining prepared

CDs with gold nanoparticles (Fig. 16b). The interaction between gold and CDs leads to fluorescence bursting of the CDs, and the incorporation of 6-thioguanine (6-TG) can form Au-S bonds with gold to release CQDs, allowing the detection of 6-TG [122].

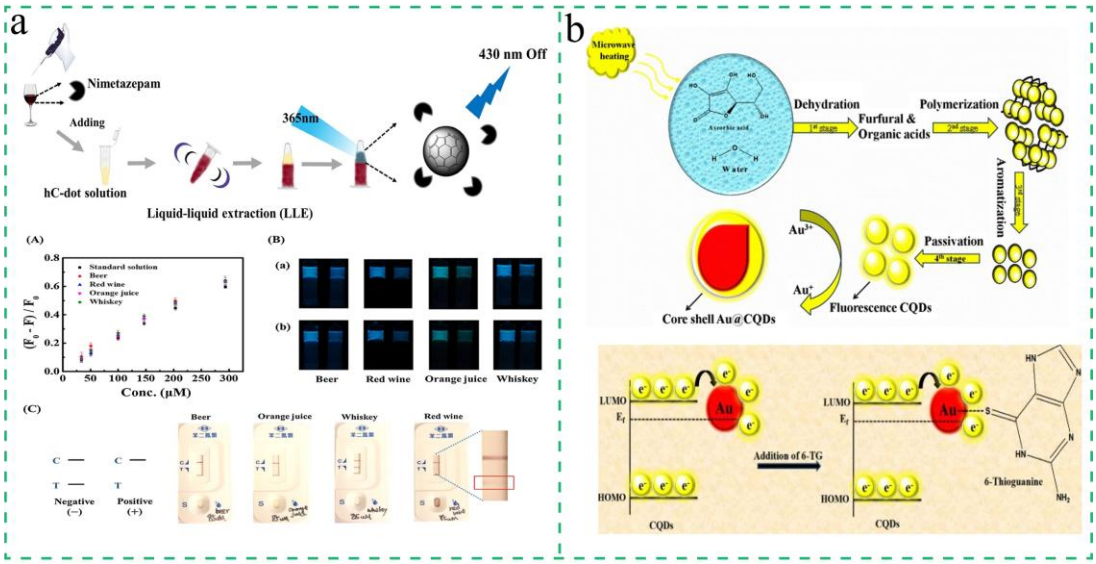

Fig. 16. (a) CDs for the analysis of drugs. Reproduced with permission from ref [121]. Copyright 2020 Elsevier. (b) Binding of CDs and gold nanoclusters for the detection of 6-TG. Reproduced with permission from ref [122]. Copyright 2018 Springer.

4.6. Applications of CDs in Imaging

Cancer is the second leading cause of death after cardiovascular disease due to untimely diagnosis, and with cancer mortality rates higher in Asia and Africa than elsewhere, there is an urgent need for rapid and accurate early diagnosis to reduce cancer deaths. The diagnosis of cancer usually requires the detection of cancer-related biomarkers such as proteins, nucleic acids, vascular endothelial growth factor (VEGF), transferrin receptor, albumin, messenger RNA and non-coding RNA. For decades, ELISA immunoassays have been the gold standard for cancer diagnosis, but this method requires labelling of the markers. In contrast, biosensors enable label-free,

rapid and portable detection of biomarkers for POCT, and the combination of biosensors with imaging assays is considered the best method for detecting cancer markers. CDs with good optical properties are widely used in imaging and can be used for biomarker sensing with simple modifications, providing impressive properties for current biosensing and imaging strategies.

In 2011, Tao et al. prepared CDs by acidifying carbon nanotubes and graphite with sulfuric and nitric acids and used them for in vivo near-infrared fluorescence imaging in animals (Fig. 17a). These CDs were characterized by bright fluorescence, low cytotoxicity and easy removal, demonstrating for the first time the great potential of CDs as non-toxic fluorescent nanoprobes. However, the low yield of CDs limits their applications in imaging [20]. In 2013, Chen et al. circumvented the limitation of low yield of CDs by preparing CDs with sucrose and oleic acid in gram-scale, achieving a yield of 41.80% [123]. Furthermore, the low toxicity of CDs makes them promising for imaging. Jiang et al. prepared blue, green and red fluorescent CDs based on different structures of phenylenediamine, which had very low cytotoxicity and remained almost non-toxic to cell when the concentration of CDs reached 50.00 μg/mL and then were used for cell imaging under 405 nm excitation, showing excellent multicolor cell imaging ability (Fig. 17b) [124]. Subsequently, researchers extended the application of CDs in cellular imaging. Li et al. prepared near-infrared fluorescent CDs at a wavelength of 700 nm using citric acid and 1,4,5,8-tetraaminoanthraquinone, which can be linked to multiple paired α-carboxylic

and amino groups on large neutral amino acid transporter proteins and selectively accumulate in human tumor xenografts and human glioma in situ mouse models (Fig. 17c). They can be loaded with anti-tumor drugs via Π-Π stacking, leading to near-infrared and photoacoustic imaging of mouse tumors, with fluorescence in the tumor region gradually increasing over time and peaking within 8 hours [125]. The integration of diagnosis and treatment can be achieved by combining highly fluorescent CDs with antimicrobial drugs, Tang et al. combined CDs with the fluorescent drug molecule adriamycin to achieve enhanced drug delivery, convenient cellular imaging, and real-time monitoring of drug release (Fig. 17d). Polyethylene glycol (PEG) was used to couple to the surface of the CDs to enhance their hydrophilicity, and DOX was loaded into the PEG lattice through electrostatic interactions and π-π stacking. When the drug DOX is on the surface of the CDs, the CDs emit weak fluorescence due to FRET, while the fluorescence intensity gradually increases with the release of DOX, allowing the intracellular drug release process to be monitored based on the change in fluorescence intensity [126]. CDs have also been used for imaging of human serum albumin (HSA), Zhang et al. prepared CDs with AIE, dual emission and solvent effect using tea saponin as the carbon source, which can be used for turn on detection of HSA and ratiometric detection of extremely acid pH (Fig. 17e). Based on the good biocompatibility and spectroscopic properties of the CDs, which were used for endogenous and exogenous HSA cellular imaging, while the drug simvastatin induced intracellular HSA production, and fluorescence

enhancement of TS-CDs by simvastatin was observed [127].

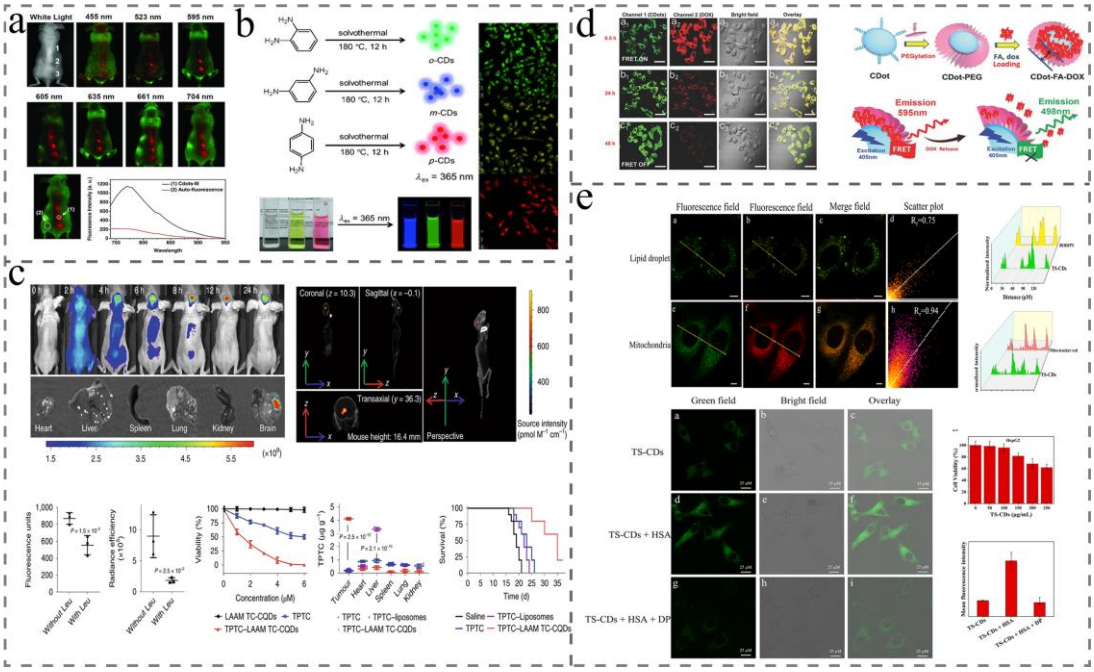

Fig. 17. (a) CDs was used in in vivo imaging for the first time. Reproduced with permission from ref [25]. Copyright 2012 Wiley-VCH. (b) Preparation of blue, green and red CDs from three different phenylenediamine isomers for multicolor imaging. Reproduced with permission from ref [124]. Copyright 2015 Wiley-VCH. (c) Near-infrared and photoacoustic imaging of tumor-bearing mice by CDs. Reproduced with permission from ref [125]. Copyright 2020 Springer Nature. (d) Simultaneous imaging of CDs and drug transport to monitor intracellular drug release processes. Reproduced with permission from ref [126]. Copyright 2013 Wiley-VCH.

CDs are very effective in photodynamic therapy and imaging (Fig. 18a). Sun et al. assembled the photosensitizers chlorine-Ce6 and Cu^{2+} with CDs, an acidic environment of tumor cell leads to an elevated glutathione (GSH) content, which can cause Cu^{2+} to leave the surface of CDs [64].Thus restoring the fluorescence of CDs based on the redox reaction between GSH and Cu^{2+}, and the CDs-Ce6 restored the therapeutic effects of PDT and PTT. Cu^{2+} oxidizes GSH to oxidized glutathione (GSSG) while catalyzing the generation of hydroxyl radicals from hydrogen peroxide H_2O_2, thereby increasing intracellular oxidative stress and enhancing the therapeutic effects of ROS. In imaging, the lower pH of tumor cell resulted in the nano system

emitting red fluorescence, which was significantly enhanced by the addition of alpha-lipoic acid, the promoter of GSH, or H_2O_2, indicating that the physiological processes described above were occurring. The anti-tumor effect of the nano system can be clearly seen in mouse imaging, with tumors treated with the Cu/CC-Ce6+light system shrinking to 89.00% of their original size within 14 days. The fluorescence imaging-guided treatment with the CDs-Ce6+light cancer system led to the development of a nanoplatform that integrates imaging and therapy.

CDs was used for lung imaging in acute lung injury. Liu et al. prepared red fluorescent CDs, whose longer wavelength (683 nm) gives them the advantages of low background interference and strong tissue penetration in bioimaging (Fig. 18b) [33]. In addition, the large number of hydroxyl, carboxyl and amino groups on its surface can bind to superoxide radicals by hydrogen bonding, promoting electron transfer and thus accelerating the disproportionation of superoxide radicals, with a catalytic activity very similar to that of natural superoxide dismutase, which is over 4,000 U/mg. The groups on its surface can scavenge harmful ROS and protect cell from oxidative stress, with an excellent therapeutic effect on lung inflammation in mice, comparable to that of the clinical drug Dexamethasone (DXMS).

Su et al. prepared panchromatic fluorescent CDs from citric acid, thiourea and ruthenium chloride, which can be used for both fluorescence imaging and X-ray computed tomography (CT) (Fig. 18c). Injection of 0.20 mL of 3.00 mg/mL CDs into mice showed a strong fluorescent signal at the tumor site and a weaker fluorescence

signal at the tumor site after 72 hours due to the greater renal clearance of CDs, demonstrating less harmful effects on the human body. In addition, CT imaging showed that the CDs was more effective than the commercial contrast agent iodixanol. In conclusion, this CDs solves the problems of poor tissue penetration and low CT sensitivity in fluorescence imaging [128].

Furthermore, the imaging of CDs has been employed to distinguish between normal and drug-resistant bacteria. Liu et al. employed a hydrothermal synthesis approach to generate NIR II region CDs (CyCDs) utilizing methanol and dopamine hydrochloride as precursors (Fig. 18d). The positive zeta potential of CyCDs enables the formation of complexes with bacteria that possess negatively charged surfaces. It is noteworthy that CyCDs only stain the cell wall of drug-resistant bacteria, whereas normal bacteria show bright fluorescence. This could be employed to identify drug-resistant bacteria in vitro, facilitating future monitoring of antibiotic [129]. In summary, CDs show great potential in imaging and, combined with their ability to act as drugs or delivery drugs, providing a powerful tool for achieving diagnostic and therapeutic integration.

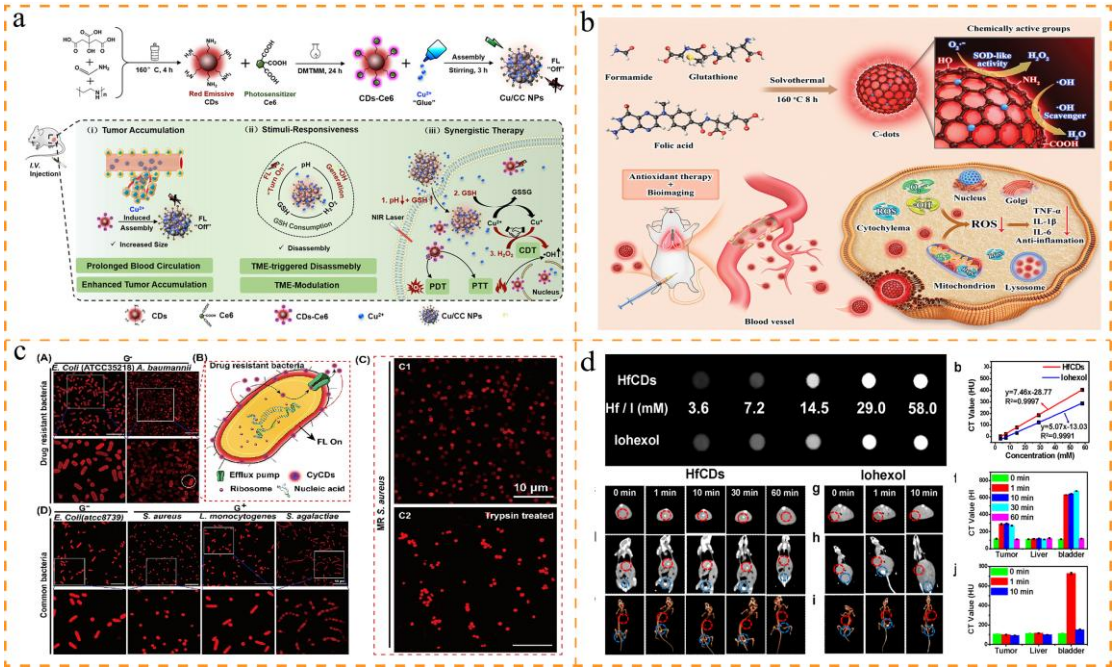

Fig. 18. (a) CDs was used in photodynamic therapy and imaging integration. Reproduced with permission from ref [64]. Copyright 2020 Wiley-VCH. (b) CDs as superoxide dismutase for bioimaging and acute lung loss therapy. Reproduced with permission from ref [33]. Copyright 2023 Wiley-VCH. (c) CDs for fluorescence and CT dual imaging of in situ hepatocellular carcinoma. Reproduced with permission from ref [128]. Copyright 2020 Elsevier. (d) Near-infrared fluorescent CDs image drug-resistant bacteria to distinguish them from normal bacteria. Reproduced with permission from ref [129]. Copyright 2023 Elsevier.

5. Conclusion and Outlook

In summary, the synthetic methods of CDs were initially reviewed, with an emphasis on the evolution of CDs synthesis from top-down to bottom-up. The traditional luminescence mechanism and emerging properties of CDs were discussed to explore the origin of fluorescence. Due to their favorable optical properties, biocompatibility, ease of modification and high stability, CDs exhibit considerable potential in the field of medicinal chemistry, including the development of nanodrugs, drug transport, drug analysis and bioimaging. Firstly, CDs were employed as antitumor, antibacterial, antiviral and neurotherapeutic agents, as well as in

photodynamic therapy and photothermal therapy. Secondly, CDs act as excellent drug carriers, facilitating the targeted delivery of various drugs to organisms, thereby address the issue of low drug uptake. Thirdly, CDs were employed as luminophores, which could be prepared as sensors by simple modification for the drug analysis and the monitoring of drug residues in the environment and human body. Finally, we presented the application of CDs in imaging for tracking drug release and studying drug pathways and metabolic processes *in vivo*.

Despite the extensive range of potential applications of CDs in medicinal chemistry and biomedicine, several challenges and limitations must be considered. Firstly, the issue of toxicity and biocompatibility is of primary concern. Although CDs have low toxicity to cell, there is a need to determine whether they produce toxic effects in complex organisms, as well as their safety in the clinical setting. A further challenge is standardization and normalization. There is considerable diversity in the preparation of CDs, resulting in incomplete consistency in the performance of CDs prepared in different laboratories. Consequently, there is a need to establish standards for CDs and performance evaluation criteria. Furthermore, for the long-term use of drugs, it is necessary to consider the biodistribution and metabolism of CDs in the body and long-term safety. In conclusion, it is expected that these challenges will progressively be addressed through continued research, thereby facilitating the wider application of CDs in the field of medicine.

CRediT Authorship Contribution Statement

Shengtao Zhang: Writing-original draft, Visualization, Investigation. **Pengyue Xu**: Writing-original draft, Visualization, Investigation. **Jiali Yang**: Visualization, Investigation. **Pengliang Song**: Writing-review & editing. **Lifang Li**: Writing-review & editing.**Yan Li**: Writing-review & editing, Supervision, Funding acquisition, Conceptualization. **Yongmin Zhang**: Writing-review & editing, Supervision. **Shaoping Wu**: Writing-review & editing, Supervision, Funding acquisition.

Declaration of Competing Interest

There are no conflicts to declare.

Acknowledgements

This work was supported by the National Natural Science Foundation of China (No. 22074119), the Key Research and Development Program of Shaanxi Province (No. 2021ZDLSF03-03), Biomedicine Key Laboratory of Shaanxi Province (No. 2018SZS41).

Abbreviations

6-TG	6-Thioguanine
ACQ	Aggregation-Caused quenching
AD	Alzheimer's disease
AEAPTMS	*N*-β-(aminoethyl)-γ-aminopropyltrimethoxysulfonate
APTES	3-aminopropyl)triethoxysilane
AHP	2-amino-3-hydroxyphenazine
AIE	Aggregation-Induced Emission
BBB	Blood-Brain Barrier
Ce6	Chlorin e6
CEE	Crosslink Enhanced Emission

CNS	Central Nervous System
CNTs	Carbon Nanotubes
CPDs	Carbonated Polymer Dots
CT	Computed Tomography
DAP	2,3-diaminophenazine
DOX	Doxorubicin
DXMS	Dexamethasone
ECL	Electrochemiluminescence
EV71	Enterovirus 71
FRET	Förster resonance energy transfer
GQDs	Graphene quantum dots
GSH	Glutathione
GSSG	Oxidized Glutathione
HepG2	Hepatocellular carcinoma
HSA	Human Serum Albumin
KSHV	Kaposi's sarcoma-associated herpesvirus
LNA	Locked Nucleic Acid
LNZ	Linezolid
MS	Mass Spectrometry
NIR	Near-infrared
NMR	Nuclear Magnetic Resonance

NPs	Nanoparticles
OPs	Organophosphorus pesticides
PDT	Photodynamic therapy
PEDV	Porcine Epidemic Diarrhea Virus
PEG	Polyethylene glycol
PRRSV	Porcine Reproductive and Respiratory Syndrome Virus
PRV	Pseudorabies virus
PT	Photothermal therapy
QCE	Quantum Confinement Effect
QDs	Quantum Dots
QYs	Quantum Yields
ROS	Reaction Oxygen Species
RTP	Room-Temperature-Phosphorescence
TOA	Time-of-Addition
VEGF	Vascular endothelial growth factor
XPS	X-ray photoelectron spectroscopy

References

[1] N. Dubey, S. Dhiman, A. Koner, Review of carbon dot-based drug conjugates for cancer therapy, ACS Appl. Nano Mater. 6 (2023), pp. 4078-4096.

[2] M. Xi, J. Zhu, F. Zhang, H. Shen, J. Chen, Z. Xiao, Y. Huang, C. Wu, H. Sun, G. Xia,

Antibody-drug conjugates for targeted cancer therapy: Recent advances in potential payloads, Eur. J. Med. Chem. 276 (2024), pp. 116709.

[3] L. Williams, M. Kolak, C. Villanueva, D. Ompad, B. Tempalski, Creation and validation of a new socio-built environment index measure of opioid overdose risk for use in both non-urban and urban settings, J Urban Health. 100 (2023), pp. 1048-1061.

[4] J. Tang, Y. Zhang, Y. Liu, D. Liu, H. Qin, N. Lian, Carbon quantum dots as a fluorophore for “inner filter effect” detection of metronidazole in pharmaceutical preparations, RSC Adv. 9 (2019), pp. 38174-38182.

[5] R. Hassan, M. Abd Maksoud, I. Ghannam, A. Azzouny, M. Enein, Synthetic non-toxic anti-biofilm agents as a strategy in combating bacterial resistance, Eur. J. Med. Chem. 262 (2023), pp. 115867.

[6] W. Zhang, G. Sigdel, K. Mintz, E. Seven, Y. Zhou, C. Wang, R. Leblanc, Carbon dots: a future blood-brain barrier penetrating nanomedicine and drug nanocarrier, Int J Nanomedicine. 16 (2021), pp. 5003-5016.

[7] Á. Serrano, K. Takayama, A. Molina, M. Seyran, S. Hassan, P. Choudhury, V. Uversky, K. Lundstrom, P. Adadi, G. Palù, A. Aljabali, G. Chauhan, R. Kandimalla, M. Tambuwala, A. Lal, T. Aziz, S. Sherchan, D. Barh, E. Redwan, N. Bazan, Y. Mishra, B. Uhal, A. Brufsky, Carbon-based nanomaterials: promising antiviral agents to combat COVID-19 in the microbial-resistant era, ACS Nano. 15 (2021), pp. 8069-8086.

[8] K. Liew, K. Chan, C. Lee, Blood–brain barrier permeable anticholinesterase aurones: synthesis, structure–activity relationship, and drug-like properties, Eur. J. Med. Chem. 94 (2015), pp. 195-210.

[9] D. Upton, C. Ung, S. George, M. Tsoli, M. Kavallaris, D. Ziegler, Challenges and opportunities to penetrate the blood-brain barrier for brain cancer therapy, Theranostics. 12 (2022), pp. 4734-4752.

[10] B. Mehrjou, Y. Wu, P. Liu, G. Wang, P. Chu, Design and properties of antimicrobial biomaterials surfaces, Adv. Healthc. Mater. 12 (2023), pp. 2202073.

[11] S. karkan, R. Arshad, A. Rahdar, A. Ramezani, R. Behzadmehr, S. Ghotekar, S. Pandey,

Recent advancements in the targeted delivery of etoposide nanomedicine for cancer therapy: A comprehensive review, Eur. J. Med. Chem. 259 (2023), pp. 115676.

[12] X. Qu, C. Gao, L. Fu, Y. Chu, J. Wang, H. Qiu, J. Chen, Positively charged carbon dots with antibacterial and antioxidant dual activities for promoting infected wound healing, ACS Appl. Mater. 15 (2023), pp. 18608-18619.

[13] K. Deng, L. Zhang, W. Gao, X. Lin, X. Long, Y. Wang, M. Wu, A functional carbon dots induce ferroptosis by suppressing PLPP4 activity to inhibit glioblastoma growth, Chem. Eng. J. 475 (2023), pp. 146473.

[14] Y. Li, X. Zheng, X. Zhang, S. Liu, Q. Pei, M. Zheng, Z. Xie, Porphyrin-based carbon dots for photodynamic therapy of hepatoma, Adv. Healthc. Mater. 6 (2017), pp. 1600924.

[15] P. Innocenzi, L. Stagi, Carbon-based antiviral nanomaterials: graphene, C-dots, and fullerenes. A perspective, Chem. Sci. 11 (2020), pp. 6606-6622.

[16] K. Cheng, H. Wang, S. Sun, M. Wu, H. Shen, K. Chen, Z. Zhang, S. Li, H. Lin, Specific chemiluminescence imaging and enhanced photodynamic therapy of bacterial infections by hemin-modified carbon dots, Small. 19 (2023), pp. 2207868.

[17] H. Fan, Z. Zhu, W. Zhang, Y. Yin, Y. Tang, X. Liang, L. Zhang, Light stimulus responsive nanomedicine in the treatment of oral squamous cell carcinoma, Eur. J. Med. Chem. 199 (2020), pp. 112394.

[18] R. Rossetti, S. Nakahara, L. Brus, Quantum size effects in the redox potentials, resonance Raman spectra, and electronic spectra of CdS crystallites in aqueous solution, J. Chem. Phys. 79 (1983), pp. 1086-1088.

[19] Y. Wang, X. Li, S. Zhao, B. Wang, X. Song, J. Xiao, M. Lan, Synthesis strategies, luminescence mechanisms, and biomedical applications of near-infrared fluorescent carbon dots, Coordin Chem Rev. 470 (2022), pp. 214703.

[20] X. Xu, R. Ray, Y. Gu, H. J. Ploehn, L. Gearheart, K. Raker, W. Scrivens, Electrophoretic analysis and purification of fluorescent single-walled carbon nanotube fragments, J. Am. Chem. Soc. 126 (2004), pp. 12736-12737.

[21] Y. Sun, B. Zhou, Y. Lin, W. Wang, K. A. Fernando, P. Pathak, M. Meziani, B. Harruff, X.

Wang, H. Wang, P. Luo, H. Yang, M. Kose, B. Chen, L. Veca, S. Xie, Quantum-sized carbon dots for bright and colorful photoluminescence, J. Am. Chem. Soc. 128 (2006), pp. 7756-7757.

[22] B. Wang, S. Lu, The light of carbon dots: From mechanism to applications, Matter. 5 (2022), pp. 110-149.

[23] T. Rasheed, Carbon dots as robust class of sustainable and environment friendlier nano/optical sensors for pesticide recognition from wastewater, Trac-Trend Aanl Chem. 160 (2023), pp. 116957.

[24] B. Zhang, C. Liu, Y. Liu, A novel one-step approach to synthesize fluorescent carbon nanoparticles, Eur. J. Inorg. Chem. 2010 (2010), pp. 4411-4414.

[25] H. Tao, K. Yang, Z. Ma, J. Wan, Y. Zhang, Z. Kang, Z. Liu, In vivo NIR fluorescence imaging, biodistribution, and toxicology of photoluminescent carbon dots produced from carbon nanotubes and graphite, Small. 8 (2012), pp. 281-290.

[26] M. Gao, C. Liu, Z. Wu, Q. Zeng, X. Yang, W. Wu, Y. Li, C. Huang, A surfactant-assisted redox hydrothermal route to prepare highly photoluminescent carbon quantum dots with aggregation-induced emission enhancement properties, Chem. Commun. 49 (2013), pp. 8015-8017.

[27] A. Krishna, C. Radhakumary, M. Antony, K. Sreenivasan, Functionalized carbon dots enable simultaneous bone crack detection and drug deposition, J Mater Chem B. 2 (2014), pp. 8626-8632.

[28] K. Holá, M. Sudolská, S. Kalytchuk, D. Nachtigallová, A. Rogach, M. Otyepka, R. Zbořil, Graphitic nitrogen triggers red fluorescence in carbon dots, ACS Nano. 11 (2017), pp. 12402-12410.

[29] H. Yang, Y. Liu, Z. Guo, B. Lei, J. Zhuang, X. Zhang, Z. Liu, C. Hu, Hydrophobic carbon dots with blue dispersed emission and red aggregation-induced emission, Nat. Commun. 10 (2019), pp. 1789.

[30] Y. Chung, C. Lee, J. Lim, J. Jang, H. Kang, C. Park, Photomodulating carbon dots for spatiotemporal suppression of alzheimer's β-Amyloid aggregation, ACS Nano. 14 (2020), pp.

16973-16983.

[31] T. Chen, T. Yao, H. Peng, A. Whittaker, Y. Li, S. Zhu, Z. Wang, An injectable hydrogel for simultaneous photothermal therapy and photodynamic therapy with ultrahigh efficiency based on carbon dots and modified cellulose nanocrystals, Adv. Funct. Mater. 31 (2021), pp. 2106079.

[32] L. Yao, M. Zhao, Q. Luo, Y. Zhang, T. Liu, Z. Yang, M. Liao, P. Tu, K. Zeng, Carbon quantum dots-based nanozyme from coffee induces cancer cell ferroptosis to activate antitumor immunity, ACS Nano. 16 (2022), pp. 9228-9239.

[33] C. Liu, W. Fan, W. Cheng, Y. Gu, Y. Chen, W. Zhou, X. Yu, M. Chen, M. Zhu, K. Fan, Q. Luo, Red emissive carbon dot superoxide sismutase nanozyme for bioimaging and ameliorating acute lung injury, Adv. Funct. Mater. 33 (2023), pp. 2213856.

[34] S. Chaitoglou, M. Sanaee, N. Aguiló-Aguayo, Bertran, Arc-discharge synthesis of iron encapsulated in carbon nanoparticles for biomedical applications, J. Nanomater. 2014 (2014), pp. 178524.

[35] C. Wang, W. Wu, A. Periasamy, H. Chang, Electrochemical synthesis of photoluminescent carbon nanodots from glycine for highly sensitive detection of hemoglobin, Green Chem. 16 (2014), pp. 2509-2514.

[36] T. Medeiros, J. Manioudakis, F. Noun, J. Macairan, F. Victoria, R. Naccache, Microwave-assisted synthesis of carbon dots and their applications, J. Mater. Chem. C. 7 (2019), pp. 7175-7195.

[37] L. Lu, Y. Zhu, C. Shi, Y. Pei, Large-scale synthesis of defect-selective graphene quantum dots by ultrasonic-assisted liquid-phase exfoliation, Carbon. 109 (2016), pp. 373-383.

[38] H. Ding, S. Yu, J. Wei, H. Xiong, Full-color light-emitting carbon dots with a surface-state-controlled luminescence mechanism, ACS Nano. 10 (2016), pp. 484-491.

[39] Z. He, Y. Sun, C. Zhang, J. Zhang, S. Liu, K. Zhang, M. Lan, Recent advances of solvent-engineered carbon dots: A review, Carbon. 204 (2023), pp. 76-93.

[40] Z. Wan, Y. Li, Y. Zhou, D. Peng, X. Zhang, J. Zhuang, B. Lei, Y. Liu, C. Hu, High-efficiency solid-state luminescence from hydrophilic carbon dots with aggregation-induced emission

characteristics, Adv. Funct. Mater. 33 (2023), pp. 2207296.

[41] K. Jiang, Y. Wang, X. Gao, C. Cai, H. Lin, Facile, quick, and gram-scale synthesis of ultralong-lifetime room-temperature-phosphorescent carbon dots by microwave irradiation, Angew. Chem. Int. Ed. 57 (2018), pp. 6216-6220.

[42] H. Li, X. He, Y. Liu, H. Huang, S. Lian, S. Lee, Z. Kang, One-step ultrasonic synthesis of water-soluble carbon nanoparticles with excellent photoluminescent properties, Carbon. 49 (2011), pp. 605-609.

[43] J. Liu, T. Kong, H. Xiong, Mulberry-leaves-derived red-emissive carbon dots for feeding silkworms to produce brightly fluorescent silk, Adv. Mater. 34 (2022), pp. 220015.

[44] Z. Zhu, R. Cheng, L. Ling, Q. Li, S. Chen, Rapid and large-scale production of multi-fluorescence carbon dots by a magnetic hyperthermia method, Angew. Chem. Int. Ed. 59 (2020), pp. 3099-3105.

[45] I. Baragau, N. Power, D. Morgan, T. Heil, R. Lobo, C. Roberts, M. Titirici, S. Dunn, S. Kellici, Continuous hydrothermal flow synthesis of blue-luminescent, excitation-independent nitrogen-doped carbon quantum dots as nanosensors, J. Mater. Chem. A. 8 (2020), pp. 3270-3279.

[46] Y. Han, B. Tang, L. Wang, H. Bao, Y. Lu, C. Guan, L. Zhang, M. Le, Z. Liu, M. Wu, machine-learning-driven synthesis of carbon dots with enhanced quantum yields, ACS Nano. 14 (2020), pp. 14761-14768.

[47] C. Chen, C. Park, B. Boudouris, J. Horng, B. Geng, C. Girit, A. Zettl, M. Crommie, R. Segalman, S. Louie, F. Wang, Controlling inelastic light scattering quantum pathways in graphene, Nature. 471 (2011), pp. 617-620.

[48] Z. Tian, X. Zhang, D. Li, D. Zhou, P. Jing, D. Shen, S. Qu, R. Zboril, A. Rogach, Full-color inorganic carbon dot phosphors for white-light-emitting diodes, Adv. Opt. Mater. 5 (2017), pp. 1700416.

[49] L. Li, L. Shi, J. Jia, D. Chang, C. Dong, S. Shuang, Fe^{3+} detection, bioimaging, and patterning based on bright blue-fluorescent N-doped carbon dots, Analyst. 145 (2020), pp. 5450-5457.

[50] Y. Song, S. Zhu, S. Zhang, Y. Fu, L. Wang, X. Zhao, B. Yang, Investigation from chemical structure to photoluminescent mechanism: a type of carbon dots from the pyrolysis of citric acid and an amine, J. Mater. Chem. C. 3 (2015), pp. 5976-5984.

[51] L. Cao, M. Zan, F. Chen, X. Kou, Y. Liu, P. Wang, Q. Mei, Z. Hou, W. Dong, L. Li, Formation mechanism of carbon dots: From chemical structures to fluorescent behaviors, Carbon. 194 (2022), pp. 42-51.

[52] S. Zhu, L. Wang, N. Zhou, X. Zhao, Y. Song, S. Maharjan, J. Zhang, L. Lu, H. Wang, B. Yang, The crosslink enhanced emission (CEE) in non-conjugated polymer dots: from the photoluminescence mechanism to the cellular uptake mechanism and internalization, Chem. Commun. 50 (2014), pp. 13845-13848.

[53] R. Wang, W. Yuan, X. Zhu, Aggregation-induced emission of non-conjugated poly(amido amine)s: Discovering, luminescent mechanism understanding and bioapplication, Chinese J Polym Sci. 33 (2015), pp. 680-687.

[54] J. Holmes, K. Ziegler, R. Doty, L. Pell, K. Johnston, B. Korgel, Highly luminescent silicon nanocrystals with discrete optical transitions, J. Am. Chem. Soc. 123 (2001), pp. 3743-3748.

[55] X. Bao, E. Ushakova, E. Liu, Z. Zhou, D. Li, D. Zhou, S. Qu, A. Rogach, On–off switching of the phosphorescence signal in a carbon dot/polyvinyl alcohol composite for multiple data encryption, Nanoscale. 11 (2019), pp. 14250-14255.

[56] J. He, Y. He, Y. Chen, X. Zhang, C. Hu, J. Zhuang, B. Lei, Y. Liu, Construction and multifunctional applications of carbon dots/PVA nanofibers with phosphorescence and thermally activated delayed fluorescence, Chem. Eng. J. 347 (2018), pp. 505-513.

[57] J. Li, H. Zhou, H. Qiu, Y. Yan, X. Wang, Z. Gao, Z. Wang, Phosphorescent carbon dots: Intermolecular interactions, properties, and applications, Coordin Chem Rev. 503 (2024), pp. 215642.

[58] Y. Liu, H. Yang, T. Huang, L. Niu, S. Liu, Recent advances of biomass-derived carbon dots with room temperature phosphorescence characteristics, Nano Today. 56 (2024), pp. 102257.

[59] C. Wang, Y. Chen, Y. Xu, G. Ran, Y. He, Q. Song, Aggregation-induced room-temperature phosphorescence obtained from water-dispersible carbon dot-based composite materials,

ACS Appl. Mater. 12 (2020), pp. 10791-10800.

[60] L. Ai, W. Xiang, J. Xiao, H. Liu, J. Yu, L. Zhang, X. Wu, X. Qu, S. Lu, Tailored fabrication of full-color ultrastable room-temperature phosphorescence carbon dots composites with unexpected thermally activated delayed fluorescence, Adv. Mater. n/a pp. 2401220.

[61] J. Li, H. Zhou, S. Jin, B. Xu, Q. Teng, C. Li, J. Li, Q. Li, Z. Gao, C. Zhu, Z. Wang, W. Su, F. Yuan, Achieving bright and long-lived aqueous room-temperature phosphorescence of carbon nitrogen dots through in situ host–guest binding, Adv. Mater. n/a pp. 2401493.

[62] S. Sun, J. Chen, K. Jiang, Z. Tang, Y. Wang, Z. Li, C. Liu, A. Wu, H. Lin, Ce6-modified carbon dots for multimodal-imaging-guided and single-NIR-laser-triggered photothermal/photodynamic synergistic cancer therapy by reduced irradiation power, ACS Appl. Mater. 11 (2019), pp. 5791-5803.

[63] Z. Li, Q. Pei, Y. Zheng, Z. Xie, M. Zheng, Carbon dots for long-term near-infrared afterglow imaging and photodynamic therapy, Chem. Eng. J. 467 (2023), pp. 143384.

[64] S. Sun, Q. Chen, Z. Tang, C. Liu, Z. Li, A. Wu, H. Lin, Tumor microenvironment stimuli-responsive fluorescence imaging and synergistic cancer therapy by carbon-dot–Cu^{2+} nanoassemblies, Angew. Chem. Int. Ed. 59 (2020), pp. 21041-21048.

[65] J. Yue, L. Li, C. Jiang, Q. Mei, W. Dong, R. Yan, Riboflavin-based carbon dots with high singlet oxygen generation for photodynamic therapy, J Mater Chem B. 9 (2021), pp. 7972-7978.

[66] Z. Wang, Z. Wang, F. Wu, Carbon dots as drug delivery vehicles for antimicrobial applications: a minireview, ChemMedChem. 17 (2022), pp. e202200003.

[67] H. Yu, X. Lv, L. Wu, B. Li, K. Huang, Y. Huang, Q. Zhang, C. Mei, X. Ren, R. Zhou, H. Luo, P. Pang, H. Shan, Doxorubicin-loaded fluorescent carbon dots with PEI passivation as a drug delivery system for cancer therapy, Nanoscale. 12 (2020), pp. 17222-17237.

[68] X. Gong, Q. Zhang, Y. Gao, S. Shuang, M. Choi, C. Dong, Phosphorus and nitrogen dual-doped hollow carbon dot as a nanocarrier for doxorubicin delivery and biological imaging, ACS Appl. Mater. 8 (2016), pp. 11288-11297.

[69] S. Kariminia, M. Shamsipur, A. Barati, Fluorescent folic acid-chitosan/carbon dot for

pH-responsive drug delivery and bioimaging, Int. J. Biol. Macromol. 254 (2024), pp. 127728.

[70] B. Ma, C. Sun, Tumor pH-triggered “charge conversion” nanocarriers with on-demand drug release for precise cancer therapy, J Mater Chem B. 8 (2020), pp. 9351-9361.

[71] N. Dubey, S. Ramteke, N. Jain, T. Dutta, A. Lal, Folate-receptor-mediated uptake of carbon dots as a pH-responsive carrier for chemotherapy, ChemistrySelect. 7 (2022), pp. e202201604.

[72] L. Yang, Z. Wang, J. Wang, W. Jiang, X. Jiang, Z. Bai, Y. He, J. Jiang, D. Wang, L. Yang, Doxorubicin conjugated functionalizable carbon dots for nucleus targeted delivery and enhanced therapeutic efficacy, Nanoscale. 8 (2016), pp. 6801-6809.

[73] L. Wang, H. Pan, D. Gu, H. Sun, K. Chen, G. Tan, W. Pan, A novel carbon dots/thermo-sensitive in situ gel for a composite ocular drug delivery system: characterization, ex-vivo imaging, and in vivo evaluation, Int. J. Mol. Sci. 22 (2021), pp. 9934.

[74] L. Hou, D. Chen, R. Wang, R. Wang, H. Zhang, Z. Zhang, Z. Nie, S. Lu, Transformable honeycomb-like nanoassemblies of carbon dots for regulated multisite delivery and enhanced antitumor chemoimmunotherapy, Angew. Chem. Int. Ed. 60 (2021), pp. 6581-6592.

[75] Q. Tan, S. Zhao, T. Xu, Q. Wang, M. Zhang, L. Yan, X. Chen, M. Lan, Inorganic nano-drug delivery systems for crossing the blood–brain barrier: advances and challenges, Coordin Chem Rev. 494 (2023), pp. 215344.

[76] X. Zhang, Q. Yu, P. Zhou, S. Yang, J. Xia, T. Deng, C. Yu, Blood-brain barrier penetrating carbon dots with intrinsic anti-inflammatory and drug-loading properties, Biomaterials Advances. 139 (2022), pp. 212995.

[77] E. Kirbas, E. Seven, Y. Zhou, B. Walters, K. Mintz, R. Pandey, A. Wikramanayake, C. Chusuei, S. Vanni, R. Graham, R. Leblanc, Metformin derived carbon dots: highly biocompatible fluorescent nanomaterials as mitochondrial targeting and blood-brain barrier penetrating biomarkers, J. Colloid Interface Sci. 592 (2021), pp. 485-497.

[78] S. Li, Z. Peng, J. Dallman, J. Baker, A. Othman, P. Blackwelder, R. Leblanc, Crossing the blood–brain–barrier with transferrin conjugated carbon dots: A zebrafish model study,

Colloids Surf. B. 145 (2016), pp. 251-256.

[79] S. Hettiarachchi, R. Graham, K. Mintz, Y. Zhou, S. Vanni, Z. Peng, R. Leblanc, Triple conjugated carbon dots as a nano-drug delivery model for glioblastoma brain tumors, Nanoscale. 11 (2019), pp. 6192-6205.

[80] M. Zheng, S. Ruan, S. Liu, T. Sun, D. Qu, H. Zhao, Z. Xie, H. Gao, X. Jing, Z. Sun, Self-targeting fluorescent carbon dots for diagnosis of brain cancer cells, ACS Nano. 9 (2015), pp. 11455-11461.

[81] S. Ohnishi, K. Takano, Amyloid fibrils from the viewpoint of protein folding, Cell. Mol. Life Sci. 61 (2004), pp. 511-524.

[82] J. Lee, D. Yang, C. Goulbourne, E. Im, P. Stavrides, A. Pensalfini, H. Chan, C. Bouchet, C. Bleiwas, M. Berg, C. Huo, J. Peddy, M. Pawlik, E. Levy, M. Rao, M. Staufenbiel, R. Nixon, Faulty autolysosome acidification in Alzheimer's disease mouse models induces autophagic build-up of Aβ in neurons, yielding senile plaques, Nat. Neurosci. 25 (2022), pp. 688-701.

[83] Y. Liu, L. Xu, Q. Wang, B. Yang, X. Zhang, Synergistic inhibitory effect of GQDs–tramiprosate covalent binding on Amyloid aggregation, ACS Chem. Neurosci. 9 (2018), pp. 817-823.

[84] Z. Wang, L. Sheng, X. Yang, J. Sun, Y. Ye, S. Geng, D. Ning, J. Zheng, M. Fan, Y. Zhang, X. Sun, Natural biomass-derived carbon dots as potent antimicrobial agents against multidrug-resistant bacteria and their biofilms, SM&T. 36 (2023), pp. e00584.

[85] S. Chen, Q. Zeng, X. Tan, M. Ye, Y. Zhang, L. Zou, S. Liu, Y. Yang, A. Liu, L. He, K. Hu, Photodynamic antibacterial chitosan/nitrogen-doped carbon dots composite packaging film for food preservation applications, Carbonhyd Polym. 314 (2023), pp. 120938.

[86] L. Wu, Y. Yang, L. Huang, Y. Zhong, Y. Chen, Y. Gao, L. Lin, Y. Lei, A. Liu, Levofloxacin-based carbon dots to enhance antibacterial activities and combat antibiotic resistance, Carbon. 186 (2022), pp. 452-464.

[87] G. Brown, D. Denning, N. Gow, S. Levitz, M. Netea, T. White, Hidden killers: human fungal infections, Sci Transl Med. 4 (2012), pp. 165rv13-165rv13.

[88] M. Thakur, S. Pandey, A. Mewada, V. Patil, M. Khade, E. Goshi, M. Sharon, Antibiotic

conjugated fluorescent carbon dots as a theranostic agent for controlled drug release, bioimaging, and enhanced antimicrobial activity, J Drug Deliv. 2014 (2014), pp. 282193.

[89] S. Ardekani, A. Dehghani, P. Ye, K. Nguyen, V. Gomes, Conjugated carbon quantum dots: potent nano-antibiotic for intracellular pathogens, J. Colloid Interface Sci. 552 (2019), pp. 378-387.

[90] R. Su, H. Yan, X. Jiang, Y. Zhang, P. Li, W. Su, Orange-red to NIR emissive carbon dots for antimicrobial, bioimaging and bacteria diagnosis, J Mater Chem B. 10 (2022), pp. 1250-1264.

[91] S. Kumari, S. Rajit, D. Mandal, P. Das, Carbon dot-DNA-protoporphyrin hybrid hydrogel for sustained photoinduced antimicrobial activity, J. Colloid Interface Sci. 553 (2019), pp. 228-238.

[92] D. Ghataty, R. Amer, M. Amer, M. Abdel, R. Shamma, Green synthesis of highly fluorescent carbon dots from bovine serum albumin for linezolid drug delivery as potential wound healing biomaterial: bio-synergistic approach, antibacterial activity, and in vitro and ex vivo evaluation, Pharmaceutics. 15 (2023), pp. 234.

[93] R. Ji, A. Barras, J. Bouckaert, N. Dumitrascu, S. Szunerits, R. Boukherroub, Enhanced antibacterial activity of carbon dots functionalized with ampicillin combined with visible light triggered photodynamic effects, Colloids Surf. B. 170 (2018), pp. 347-354.

[94] Y. Liu, X. Liu, Y. Xiao, F. Chen, F. Xiao, A multifunctional nanoplatform based on mesoporous silica nanoparticles for imaging-guided chemo/photodynamic synergetic therapy, RSC Adv. 7 (2017), pp. 31133-31141.

[95] S. Liu, K. Lv, Z. Chen, C. Li, T. Chen, D. Ma, Fluorescent carbon dots with a high nitric oxide payload for effective antibacterial activity and bacterial imaging, Biomater. Sci. 9 (2021), pp. 6486-6500.

[96] A. Pramanik, S. Jones, F. Pedraza, A. Vangara, C. Sweet, M. Williams, V. Ruppa, S. Risher, D. Sardar, P. Ray, Fluorescent, magnetic multifunctional carbon dots for selective separation, identification, and eradication of drug-resistant superbugs, ACS Omega. 2 (2017), pp. 554-562.

[97] C. Lin, L. Chang, H. Chu, H. Lin, P. Chang, R. Wang, B. Unnikrishnan, J. Mao, S. Chen, C. Huang, High amplification of the antiviral activity of curcumin through transformation into carbon quantum dots, Small. 15 (2019), pp. 1902641.

[98] T. Tong, H. Hu, J. Zhou, S. Deng, X. Zhang, W. Tang, L. Fang, S. Xiao, J. Liang, Glycyrrhizic-acid-based carbon dots with high antiviral activity by multisite inhibition mechanisms, Small. 16 (2020), pp. 1906206.

[99] D. Ting, N. Dong, L. Fang, J. Lu, J. Bi, S. Xiao, H. Han, Multisite inhibitors for enteric coronavirus: antiviral cationic carbon dots based on curcumin, ACS Appl. Nano Mater. 1 (2018), pp. 5451-5459.

[100] E. Ju, T. Li, Z. Liu, S. Silva, S. Wei, X. Zhang, X. Wang, S. Gao, Specific inhibition of viral microRNAs by carbon dots-mediated delivery of locked nucleic acids for therapy of virus-induced cancer, ACS Nano. 14 (2020), pp. 476-487.

[101] J. Cheng, Y. Xu, D. Zhou, K. Liu, N. Geng, J. Lu, Y. Liu, J. Liu, Novel carbon quantum dots can serve as an excellent adjuvant for the gp85 protein vaccine against avian leukosis virus subgroup J in chickens, Poultry Sci. 98 (2019), pp. 5315-5320.

[102] D. Iannazzo, A. Pistone, S. Ferro, L. Luca, A. Monforte, R. Romeo, M. Buemi, C. Pannecouque, graphene quantum dots based systems as HIV inhibitors, Bioconjug. Chem. 29 (2018), pp. 3084-3093.

[103] A. Mohammadinejad, K. Abnous, M. Alinezhad, R. Yahyazadeh, S. Hamrah, F. Senobari, S. Mohajeri, Application of green-synthesized carbon dots for imaging of cancerous cell lines and detection of anthraquinone drugs using silica-coated CdTe quantum dots-based ratiometric fluorescence sensor, Spectrochim. Acta. A. 288 (2023), pp. 122200.

[104] Y. Zhong, A. Chen, X. Yin, R. Li, Q. Deng, R. Yang, Red emission carbon dots for mitoxantrone detection, Sens. Actuators B Chem. 382 (2023), pp. 133535.

[105] A. Rateb, Z. Ghubish, A. Abdel, M. El-Kemary, A multifunctional sensing of two carbon dots based on diaminonaphthalenes for detection of ofloxacin drug, J. Photochem. 443 (2023), pp. 114867.

[106] J. Zhang, Y. Li, L. Teng, Y. Cao, X. Hu, G. Fang, S. Wang, A molecularly imprinted

fluorescence sensor for sensitive detection of tetracycline using nitrogen-doped carbon dots-embedded zinc-based metal-organic frameworks as signal-amplifying tags, Anal. Chim. Acta. 1251 (2023), pp. 341032.

[107] K. Wang, Q. Ji, J. Xu, H. Li, D. Zhang, X. Liu, Y. Wu, H. Fan, Highly sensitive and selective detection of amoxicillin using carbon quantum dots derived from Beet, J. Fluoresc. 28 (2018), pp. 759-765.

[108] Q. Wang, Q. Tan, S. Zhao, K. Zhang, J. Chen, M. Lan, Dual-responsive carbon dots-based luminophore for ratiometric fluorescence and room-temperature phosphorescence detection of oxytetracycline, Chem. Eng. J. 470 (2023), pp. 144061.

[109] Y. Zhu, J. Li, Z. Yan, N. Zhao, X. Yang, Developing Carbon Dots with Room-Temperature Phosphorescence for the Dual-Signal Detection of Metronidazole, Langmuir. 38 (2022), pp. 15442-15450.

[110] Z. Li, S. Li, L. Jiang, J. Xiao, J. Niu, Y. Zhang, C. Chen, Q. Zhou, Construction of nitrogen-doped carbon dots-based fluorescence probe for rapid, efficient and sensitive detection of chlortetracycline, Chemosphere. 361 (2024), pp. 142535.

[111] Y. Guo, J. Liu, Y. Chen, Y. Chai, Z. Li, R. Yuan, Boron and nitrogen-codoped carbon dots as highly efficient electrochemiluminescence emitters for ultrasensitive detection of Hepatitis B virus DNA, Anal. Chem. 94 (2022), pp. 7601-7608.

[112] J. Liu, Y. Zhang, R. Yuan, Y. Chai, Fluorine-nitrogen co-doped carbon dots with stable and strong electrochemiluminescence as an emitter for ultrasensitive detection of HIV-DNA fragment, Sens. Actuators B Chem. 379 (2023), pp. 133260.

[113] Y. Wang, C. Deng, S. Qian, H. Li, P. Fu, H. Zhou, J. Zheng, An ultrasensitive lateral flow immunoassay platform for foodborne biotoxins and pathogenic bacteria based on carbon-dots embedded mesoporous silicon nanoparticles fluorescent reporter probes, Food Chem. 399 (2023), pp. 133970.

[114] L. Xu, J. Zhu, S. Ding, Immunoassay of SARS-CoV-2 nucleocapsid proteins using novel red emission-enhanced carbon dot-based silica spheres, Analyst. 146 (2021), pp. 5055-5060.

[115] M. Deka, P. Dutta, S. Sarma, O. Medhi, N. Talukdar, D. Chowdhury, Carbon dots derived

from water hyacinth and their application as a sensor for pretilachlor, Heliyon. 5 (2019), pp. e01985.

[116] S. Lan, X. Wang, Q. Liu, J. Bao, M. Yang, H. Fa, C. Hou, D. Huo, Fluorescent sensor for indirect measurement of methyl parathion based on alkaline-induced hydrolysis using N-doped carbon dots, Talanta. 192 (2019), pp. 368-373.

[117] B. Lin, Y. Yan, M. Guo, Y. Cao, Y. Yu, T. Zhang, Y. Huang, D. Wu, Modification-free carbon dots as turn-on fluorescence probe for detection of organophosphorus pesticides, Food Chem. 245 (2018), pp. 1176-1182.

[118] H. Li, D. Su, H. Gao, X. Yan, D. Kong, R. Jin, X. Liu, C. Wang, G. Lu, Design of red emissive carbon dots: robust performance for analytical applications in pesticide monitoring, Anal. Chem. 92 (2020), pp. 3198-3205.

[119] S. Hiremath, B. Priyadarshi, M. Banerjee, A. Chatterjee, Carbon dots-MnO_2 based turn-on fluorescent probe for rapid and sensitive detection of hydrazine in water, J. Photochem. 389 (2020), pp. 112258.

[120] L. Chen, J. Lu, M. Luo, H. Yu, X. Chen, J. Deng, X. Hou, E. Hao, J. Wei, P. Li, A ratiometric fluorescent sensing system for the selective and ultrasensitive detection of pesticide residues via the synergetic effects of copper nanoclusters and carbon quantum dots, Food Chem. 379 (2022), pp. 132139.

[121] Y. Yen, Y. Lin, T. Chen, S. Chyueh, H. Chang, A carbon-dot sensing probe for screening of date rape drugs: nitro-containing benzodiazepines, Sens. Actuators B Chem. 305 (2020), pp. 127441.

[122] A. Mehta, A. Mishra, S. Basu, Optical detection of thiol drugs by core–shell luminous carbon dots—gold nanoparticles system, Plasmonics. 13 (2018), pp. 2239-2248.

[123] B. Chen, F. Li, S. Li, W. Weng, H. Guo, T. Guo, X. Zhang, Y. Chen, T. Huang, X. Hong, S. You, Y. Lin, K. Zeng, S. Chen, Large scale synthesis of photoluminescent carbon nanodots and their application for bioimaging, Nanoscale. 5 (2013), pp. 1967-1971.

[124] K. Jiang, S. Sun, L. Zhang, Y. Lu, A. Wu, C. Cai, H. Lin, Red, green, and blue luminescence by carbon dots: full-color emission tuning and multicolor cellular imaging, Angew. Chem. Int.

Ed. 54 (2015), pp. 5360-5363.

[125] S. Li, W. Su, H. Wu, T. Yuan, C. Yuan, J. Liu, G. Deng, X. Gao, Z. Chen, Y. Bao, F. Yuan, S. Zhou, H. Tan, Y. Li, X. Li, L. Fan, J. Zhu, A. Chen, F. Liu, Y. Zhou, M. Li, X. Zhai, J. Zhou, Targeted tumour theranostics in mice via carbon quantum dots structurally mimicking large amino acids, Nat Biomed Eng. 4 (2020), pp. 704-716.

[126] J. Tang, B. Kong, H. Wu, M. Xu, Y. Wang, Y. Wang, D. Zhao, G. Zheng, Carbon nanodots featuring efficient FRET for real- time monitoring of drug delivery and two- photon imaging, Adv. Mater. 25 (2013), pp. 6569-6574.

[127] S. Zhang, B. Li, J. Zhou, J. Shi, Z. He, Y. Zhao, Y. Li, Y. Shen, Y. Zhang, S. Wu, Kill three birds with one stone: Mitochondria-localized tea saponin derived carbon dots with AIE properties for stable detection of HSA and extremely acidic pH, Food Chem. 405 (2023), pp. 134865.

[128] Y. Su, S. Liu, Y. Guan, Z. Xie, M. Zheng, X. Jing, Renal clearable hafnium-doped carbon dots for CT/fluorescence imaging of orthotopic liver cancer, Biomaterials. 255 (2020), pp. 120110.

[129] W. Liu, B. Wu, W. Sun, W. Liu, H. Gu, J. Du, J. Fan, X. Peng, Near-infrared II fluorescent carbon dots for differential imaging of drug-resistant bacteria and dynamic monitoring of immune system defense against bacterial infection in vivo, Chem. Eng. J. 471 (2023), pp. 144530.